CR 137620
AVAILABLE TO THE PUBLIC

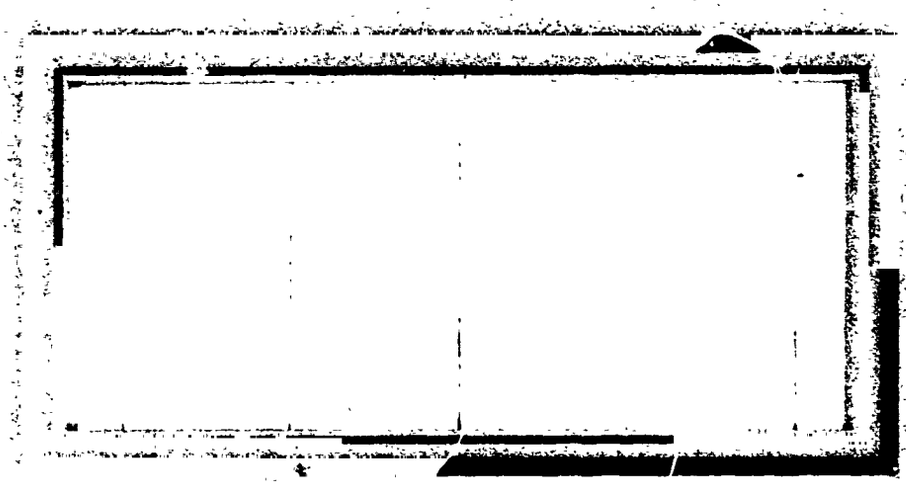

(NASA-CR-137620) THEORETICAL STUDIES ON TONE NOISE FROM A DUCTED FAN ROTOR (Rao and Associates, Inc., Palo Alto, Calif.) 69 p HC $4.25 CSCL 20A

N75-14764

Unclas

G3/07 07948

RAO AND ASSOCIATES, INC.

460 San Antonio Road
Palo Alto CA 94306
Phone: (415) 494-1695

CR 137620

THEORETICAL STUDIES ON TONE NOISE FROM A DUCTED FAN ROTOR

by

G. V. R. Rao

W. T. Chu

R. V. Digumarthi

R. K. Agarwal

September, 1974

RAO AND ASSOCIATES, INC.

PALO ALTO, CALIFORNIA
94306

PREFACE

This report presents investigations carried out by Rao and Associates for the National Aeronautics and Space Administration, Ames Research Center, Moffett Field, California under Contract NAS 2-6401. Together with earlier reports NASA CR-114576 and NASA CR-2354, this report describes the results of analytical studies on fan noise conducted under the contract. The helpful suggestions by Mr. B. K. Hodder and Mr. D. H. Hickey, the technical managers on this contract, are greatly appreciated.

SUMMARY

The method of computing radiated noise from a ducted rotor due to inflow distortion and turbulence are examined. Analytical investigations include an appropriate description of sources, the cut-off conditions imposed on the modal propagation of the pressure waves in the annular duct, and reflections at the upstream end of the duct. Far field sound pressure levels at blade passing frequency due to acoustic radiation from a small scale low speed fan are computed. Theoretical predictions are in reasonable agreement with experimental measurements.

TABLE OF CONTENTS

LIST OF SYMBOLS

B	number of blades
V	mean relative velocity met by rotor blades
N	rotor revolutions per second
P	far field pressure
U	mean axial inflow velocity
R	distance of field point from center of duct inlet
$\vec{D}$	dipole distribution in the rotor region
S	monopole distribution in the rotor region
r	radial coordinate
θ	angle measured from a reference meridional plane, positive in the direction of rotor rotation
z	axial coordinate along the rotor axis measured positive from the mid-chord plane in downstream direction
b	blade thickness
t	time
u	axial acoustic particle velocity
p	acoustic pressure
$u_c, u_\perp$	velocity fluctuations along and normal to blade chord
k	wave number of the radiated sound
ℓ	duct length upstream of rotor
c	blade-chord length
a_o	ambient speed of sound

l lift distribution along the chord per unit span per unit chord length

s monopole distribution along blade chord

Φ spectral density function

Ω rotor circular frequency

χ specific modal impedence

Ψ azimuthal angle

λ blade stagger angle

γ vorticity distribution along the blade chord

ρ_o ambient air density

υ circular frequency of the radiated sound

ν circular frequency of convected sinusoidal gust met by the rotor blade

ν_R reduced frequency of the convected sinusoidal gust

ζ distance along the blade chord from mid chord, positive toward trailing edge

η distance perpendicular to the blade chord

$\zeta^{\mu}_{m\nu}$ radiation impedence of the open end of the duct

Subscripts

h at hub

t at tip

b due to blade thickness

ℓ due to blade loading

j refers to the jth blade

Superscripts

$\overline{}$	temporal mean
$\hat{}$	amplitude
+	propagation towards the rotor
-	propagation towards the open end of the duct
*	complex conjugate
i	equivalent incompressible plane
s	due to monopole radiation
d	due to dipole radiation

1.0 INTRODUCTION

Fan noise sources and acoustic radiation from them have been the subject of analytical studies at Rao and Associates, Inc., under Contract No. NAS2-6401 with Ames Research Center of the National Aeronautics and Space Administration. The results of previous studies reported in Ref. (1) and experimental data reported in Ref. (2) have well established that disturbances in the inflow to the rotor play a primary role in noise generation. The theoretical predictions on fan rotor noise presented in Ref. (1) were based on radiation to far field from the acoustic sources in the rotor region ignoring any duct effects. The present report includes the effect of the annular duct enclosing the rotor.

In the experiments carried out in the anechoic chamber at Ames Research Center on the small scale fan shown in Figure 1 and reported in Ref. (2), the annular duct entrance is 14 in. (35.56 cm) upstream of the rotor, whereas on the downstream side, the duct is extended straight through the chamber wall to the exterior of the chamber. To take into account the influence of the duct configuration, we extended our analysis to include modal propagation of acoustic waves in a duct extending to infinity downstream of the rotor but terminated upstream at a finite distance from the rotor, as sketched in Fig. 1.

In our analysis, first we describe the typical features of the nature of the inflow to the ducted rotor in Section 2. The steady state non-uniformity as well as the turbulent velocity fluctuations in the inflow give rise to acoustic sources in the rotor region as discussed in Section 3. Dipole sources due to fluctuating lift forces on the blades and monopole sources due to finite thickness of the blades are determined in this chapter. Acoustic propagation from these sources is described in Section 4, considering the effect of the annular duct on the circumferential and radial modes of the propagating pressure waves. The influence of the upstream end of the duct on each mode is examined by assuming that the duct is terminated by a flange extending transversely to infinity. Since acoustic energy is transmitted through the duct only by the axial component of acoustic particle velocity, we considered only the axial component of particle velocity in the pressure waves. Taking into account the reflections of the duct modes from the duct entrance, farfield sound radiation is derived in this Section. Theoretical relations developed in Sections 2 to 4 are used in predicting acoustic radiation from the small scale fan rotor and the computational results are discussed in Section 5. Comparison with experimental measurements on the small scale fan in the anechoic chamber at NASA-Ames Research Center indicates some improvements that can be made in the analytic

predictions. Conclusions drawn from general features of noise propagation from ducted fan rotors are given in Section 6. Recommendations for future effort in theoretical prediction of fan noise are also described in this section.

2.0 . DESCRIPTION OF TURBULENT FLOW FIELD IN THE DUCT

The flow in the duct upstream of rotor contains random as well as deterministic fluctuations as discussed in Ref. (1). Our present interest being in the interaction of inflow turbulence with rotor blades, we postulate a suitable description of turbulent velocity fluctuations along and perpendicular to the blade chord. Let u_c and $u_\perp$ denote these velocity components which can be described in terms of their mean square values and spectral densities.

Since at any instant of time, the instantantaneous velocity fluctuations $u_c(r,\theta,z,t)$ and $u_\perp(r,\theta,z,t)$ must have a unique value when the azimuthal angle θ is increased by any multiple of 2π, we expand u_c and $u_\perp$ in a Fourier series in θ as

$$\begin{Bmatrix} u_c(r,\theta,z,t) \\ u_\perp(r,\theta,z,t) \end{Bmatrix} = \sum_g \begin{Bmatrix} u_{c,g}(r,z,t) \\ u_{\perp,g}(r,z,t) \end{Bmatrix} \cdot e^{-ig\theta} \cdot e^{-i\phi_g} \qquad (2.1)$$

where $u_{c,g}$ and $u_{\perp,g}$ are complex and random functions with respect to time t. Now, under the assumption of homogeneous frozen convected turbulence, $u_{c,g}$ and $u_{\perp,g}$ can be written in terms of their Fourier transforms

$$\begin{Bmatrix} u_{c,g}(r,z,t) \\ u_{\perp,g}(r,z,t) \end{Bmatrix} = \int_{-\infty}^{\infty} \begin{Bmatrix} \hat{u}_{c,g}(r,\omega) \\ \hat{u}_{\perp,g}(r,\omega) \end{Bmatrix} e^{-i\omega(t-z/U)} \cdot d\omega \qquad (2.2)$$

It is important to note here that Eq. (2.2) is only a symbolic representation of the random quantities u_c and $u_\perp$. The only physically meaningful results are the mean square values $\overline{u_c^2}$ and $\overline{u_\perp^2}$.

The space time correlation function $R(\xi,\eta,\zeta,\tau)$ of velocity components $u_\perp$ and u_c for frozen convected homogeneous turbulence is assumed to be of the separable form as

$$R(\xi,\eta,\zeta,\tau) = f_{\xi,\tau} \cdot f_\eta \cdot f_\zeta \tag{2.3}$$

where ξ,η,ζ denote the separation distances along the axial, circumferential, and radial directions respectively and τ denotes the separation time. We further assume that the correlation function in the axial and circumferential directions is of exponential form while in the radial direction it is unity within the correlation length and zero outside, that is the "eddy" is perfectly correlated in the radial direction. Since the turbulence is frozen convected with velocity U in the axial direction,

$$f_{\xi,\tau} = \exp\{|\xi - U\,\tau|/\ell_z\} \tag{2.4}$$

where ℓ_z is the correlation length in the axial direction. Since

the correlation function must be periodic in the circumferential direction, we write

$$f_\eta = \sum_{g=-\infty}^{\infty} \exp\{- |\eta + g\, 2\pi r|/\ell_\theta\}$$

where ℓ_θ is the correlation length in the circumferential direction. Using Poisson Summation formula (Ref. 3), the summation over g is transformed into a complex Fourier series to yield

$$f_\eta = \sum_{g} \frac{\ell_0/\pi r}{1 + (g\ell_\theta/r)^2} \cdot \exp(-ig\eta/r) \qquad (2.5)$$

In order to be consistent with the assumption that the correlation function is separable, the ratio (ℓ_θ/r) has to be considered constant with radius. Noting that $\eta = r\theta$, Eq. (2.5) can be written as

$$f_\eta = \sum_{g} \frac{(\ell_\theta/\pi r)}{1 + (g\ell_\theta/r)^2} \exp(-ig\theta) \qquad (2.6)$$

The correlation function f_ζ in the radial direction is assumed as

$$\begin{aligned} f_\zeta &= 1 \quad \text{for } 0 \leq \zeta \leq \ell_r \\ &= 0 \quad \text{for } \zeta > \ell_r \end{aligned} \qquad (2.7)$$

Since the correlation function must be unity when ξ, η, ζ and τ all are zero, the Eq. (2.3) is normalized by dividing it by a factor

$$\sum_{g=-\infty}^{\infty} \frac{(\ell_\theta/\pi r)}{1 + (g\ell_\theta/r)^2} = \coth(\pi r/\ell_\theta)$$

and we obtain

$$R(\xi,\eta,\zeta,\tau) = \exp\{|\xi - U\tau|/\ell_z\} \times \tanh\{\pi r/\ell_\theta\} \cdot \sum_g \frac{(\ell_\theta/\pi r)}{1 + (g\ell_\theta/r)^2} \cdot \exp(-ig\theta) \tag{2.8}$$

Measurements at inlet of the small scale fan indicated longitudinal correlation length ℓ_z to be same for both components $u_\perp$ and u_θ. In the absence of specific measurements to the contrary we can consider that ℓ_θ is also the same, leading us to to a reasonable assumption that above Eq. (2.8) gives the correlation function for both the velocity components $u_\perp$ and u_c.

Now the power spectral density functions $\phi_{u_c}(\omega)$ and $\phi_{u_\perp}(\omega)$ can be evaluated by taking the Fourier transform of the correlation function, and we obtain

$$\begin{Bmatrix} \Phi_{u_c} \\ \Phi_{u_\perp} \end{Bmatrix} = \begin{Bmatrix} \overline{u_c^2} \\ \overline{u_\perp^2} \end{Bmatrix} \frac{\ell_z/\pi U}{1 + (\ell_z \omega/U)^2}$$

$$\times \sum_{g=-\infty}^{\infty} \tanh \{\pi r/\ell_\theta\} \cdot \frac{\ell_\theta/\pi r}{1 + (g\ell_\theta/r)^2} \qquad (2.9)$$

where $\overline{u_c^2}$, $\overline{u_\perp^2}$ respectively are mean square values of the fluctuations along and normal to the blade chord.

The spectral density of u_c given above differs from that employed in our earlier work reported in Ref. (1), since in our present approach, we have assumed the same correlation function for u_c and $u_\perp$ components. We also note that, due to the exponential form of f_η assumed here, the gth component of above equation is different from that employed in Ref. 1.

3.0 ACOUSTIC SOURCES IN THE ROTOR REGION

The interaction of velocity fluctuations described by Eq. (2.2) with rotor blades gives rise to mass fluctuations (due to blade thickness) and fluctuating lift forces in the rotor region. These mass fluctuations and force fluctuations give rise to the so-called "aerodynamically generated noise" and can be replaced by corresponding monopole and dipole distributions respectively in the same manner as described in Ref. (1).

The velocity field described by Eq. (2.2) is in the duct coordinate system, and the velocity fluctuations as met by the rotating blade are described in the following section. In section 3.2, the influence of these velocities on the blades and the resulting distribution of acoustic sources in the rotor region are evaluated. The analyses reported here differs from that reported in Ref. 1 in that we have included the effect of compressibility and also considered chord-wise distribution of lift loading on the rotor blades.

3.1 Flow fluctuations met by the rotor blades:

For the sake of convenience, it assumed that the mid-chords of the rotor blades lie in the plane $z = 0$. Let us denote the blade, whose mid-chord occupies the position $\theta = 0$ at time $t = 0$, as the first blade. Measuring θ positive in the direction of rotor rotation

and counting the blades in the same sense, the mid-chord of the jth blade occupies the position

$$\theta_j = 2\pi\frac{j-1}{B} \quad \text{at time } t = 0$$

Thus the coordinates of a point on the chord of the jth blade at a distance ζ rearward from its mid-chord at time t can be written as

$$(r_\zeta;\ \theta_{j,\zeta} = \Omega t + 2\pi\frac{j-1}{B} - \frac{\zeta \sin\lambda}{r};\quad z_\zeta = \zeta\cos\lambda) \qquad (3.1)$$

where

Ω = circular frequency of the rotor, and

λ = blade stagger angle

The leading and trailing edges of the blade section are given by $\zeta = -c/2$ and $c/2$ respectively. The coordinates r_ζ and z_ζ in Eq. (3.1) are not subscripted by j since they do not depend upon the specific blade.

Since the circumferential velocity Ωr of the blade element is independent of time, the fluctuations met by the element at ζ on the jth blade can be written as

$$\begin{Bmatrix} u_c(r_\zeta, \theta_{j,\zeta}, z_\zeta, t) \\ u_\perp(r_\zeta, \theta_{j,\zeta}, z_\zeta, t) \end{Bmatrix}$$

$$= \sum_g \int_{-\infty}^{\infty} \begin{Bmatrix} u_{c,g}(r,\omega) \\ u_{\perp,g}(r,\omega) \end{Bmatrix} \cdot e^{-i\phi_g} \cdot \exp\{-i\omega\ (t - \xi \cos\lambda/U\ )\}$$

$$\times \exp\{-ig(\Omega t + 2\pi\frac{j-1}{B} - \frac{\zeta \sin\lambda}{r})\}d\omega \qquad (3.2)$$

In terms of the relative velocity V met by the blade, we can write

$$\frac{\zeta \sin\lambda}{r} = \frac{\Omega\zeta}{V}$$

$$\frac{\zeta \cos\lambda}{U} = \frac{\zeta}{V} \qquad (3.3)$$

Substituting relations (3.3) in (3.2), we obtain the gth component of velocity fluctuations as

$$\begin{Bmatrix} u_{c,g} \\ u_{\perp,g} \end{Bmatrix} = \int_{-\infty}^{\infty} \begin{Bmatrix} \hat{u}_{c,g}(r,\omega\ ) \\ \hat{u}_{\perp,g}(r,\omega\ ) \end{Bmatrix} e^{-i\phi_g} \cdot \exp\{-i_g 2\pi\frac{j-1}{B}\}$$

$$\times \exp\{-i\ (g\Omega + \omega\ )\ (t - \frac{\zeta}{V})\}d\omega \qquad (3.4)$$

3.2 Evaluation of source distributions:

In determining the effect of fluctuating flow on the rotor blades and the resulting monopole and dipole distributions, we make the following assumptions:

(1) Each blade section is considered as an element of an isolated airfoil immersed in a "two-dimensional flow" corresponding to the conditions occuring at the blade section.

(2) Only the velocity fluctuations parallel to the chord are significant in evaluating monopole distribution due to mass flow fluctuations. Similarly, the velocity fluctuations perpendicular to the chord are important in evaluating the dipole distribution due to blade lift.

(3) The flowfield is considered irrotational and inviscid, in spite of the fact that the velocity fluctuations u_c and $u_\perp$ described by Eq. (3.4) do not satisfy the irrotationality condition. It is assumed that the small vorticity in the flow does not affect the source distribution for a thin airfoil. (Ref. 4).

With the above assumptions, the governing equation for the perturbation velocity potential due to relative velocity V past the blade is

$$\frac{1}{a_o^2}\phi_{tt} + \frac{2M}{a_o}\phi_{\zeta t} + M^2\phi_{\zeta\zeta} = \phi_{\zeta\zeta} + \phi_{\eta\eta} \qquad (3.5)$$

where a_o is the speed of sound; $M = V/a_o$; ζ and η are the coordinates in direction parallel and perpendicular to the blade-chord respectively.

Applying Lorentz transformation

$$\zeta = \beta\bar{\zeta}\ ;\ \eta = \bar{\eta},\quad t = \{\bar{t} - M\zeta/a_o\}/\beta\ ;\quad \beta^2 = 1-M^2\ ,$$

above equation can be transformed into the wave equation

$$\frac{1}{a_o^2}\cdot\Phi_{\bar{t}\,\bar{t}} = \Phi_{\bar{\zeta}\,\bar{\zeta}} + \Phi_{\bar{\eta}\,\bar{\eta}} \qquad (3.6)$$

where $\Phi = \beta\phi$

In order to obtain simple closed form expressions for the source distributions (monopole and dipole) we follow Osborne's approach (Ref. 5) which converts the compressible flow problem into an equivalent incompressible plane in the region close to the airfoil (inner region) using the method of matched asymptotic expansions under the assumption

$$\{\varepsilon/\beta^2\}^2 << 1 \qquad (3.7)$$

where $\varepsilon = \frac{\nu c}{4\pi a_o}$, $\nu = \text{gust}$

This is accomplished by defining a new set of variables in the incompressible plane (in the inner region) as follows:

$$\zeta^i,\ \eta^i = \frac{\bar{\zeta},\ \bar{\eta}}{c/2\beta};\quad t^i = \frac{\nu \bar{t}}{2\pi\beta};\ \Phi^i = \frac{\Phi}{\{\nu c^2/8\pi\beta^3\}}$$

the equation (3.7) then becomes

$$\Phi^i_{\zeta^i\zeta^i} + \Phi^i_{\eta^i\eta^i} = \{\epsilon/\beta^2\}^2 \Phi^i_{t^i t^i}$$

which is approximated as

$$\Phi^i_{\zeta^i\zeta^i} + \Phi^i_{\eta^i\eta^i} = 0 \qquad (3.8)$$

under the assumption Eq. (3.7).

It should be noted here that the boundary conditions applicable for the solution of Eq.(3.8) are those in the inner region only. Thus, Eq.(3.8) is required to be solved with boundary conditions on the airfoil only.

The expressions given in Eq. (3.4) for the gth component of chordwise and vertical velocity fluctuations, using the above transformations, become

$$\begin{Bmatrix} u^i_{c,g} \\ u^i_{\perp,g} \end{Bmatrix} = \frac{1}{\Omega} \int_{-\infty}^{\infty} (g\Omega+\omega) \begin{Bmatrix} \hat{u}^i_{c,g}(\omega) \\ \hat{u}^i_{\perp,g}(\omega) \end{Bmatrix} e^{-i\phi_g} \cdot \exp\{-ig2\pi\tfrac{j-1}{B}\}$$

$$\times \exp\{-i\nu^i(t^i - \zeta^i/V^i)\}\, d\omega \qquad (3.9)$$

where

$$\nu^i = 2\pi;\ V^i = 4\pi\beta^2 V/\nu c$$

$$\begin{Bmatrix} u^i_{c,g} \\ u^i_{s,g} \end{Bmatrix} = (4\pi\beta^3/\Omega c) \begin{Bmatrix} \beta u_{c,g} \\ u_{s,g} \end{Bmatrix}$$

$$\begin{Bmatrix} \hat{u}^i_{c,g} \\ \hat{u}^i_{s,g} \end{Bmatrix} = (4\pi\beta^3/\nu c) \begin{Bmatrix} \beta\, \hat{u}_{c,g} \\ \hat{u}_{s,g} \end{Bmatrix}$$

and $\nu = g\Omega+\omega$

(a) Mass Flow fluctuations and resulting Monopole Sources:

A rotor blade subjected to chord-wise velocity fluctuations can be represented by a fluctuating distribution of volume sources along the blade chord. The volume sources on each blade, representing the blade profile, are obtained by solving the equivalent incompressible flow problem and then transforming the result to the compressible case. We therefore first solve Eq. (3.8) subject to the following continuity equation.

$$\left\{ \frac{d}{d\zeta}\ b(V + u_{c,g}\ + \partial\phi/\partial\zeta) = \partial\phi/\partial\eta \right\}^i \quad \text{at } \eta = 0$$

$$\text{on. } -c^i/2 \leq \zeta^i \leq c^i/2 \qquad (3.11)$$

where $b(\zeta)$ is the thickness distribution along the chord. The notation $\{\ \}^i$ implies that the boundary condition is to be transformed into the incompressible plane.

Since we are interested in the noise generated due to unsteady fluctuations only, we omit the contribution due to steady state velocity V. Also assuming that

$\frac{\partial \phi}{\partial \zeta} << u_{c,g}$ the continuity equation (3.11) can be simplified to

$$\left\{ \frac{\partial \phi}{\partial \eta} \Big|_{\eta = 0} = \frac{1}{2} \frac{d}{d\zeta} (b \cdot u_{c,g}) \right\}^i \quad \text{on } -c^i/2 \leq \zeta^i \leq c^i/2$$

$$\text{or } \frac{\partial \phi^i}{\partial \eta^i} \Big|_{\eta^i = 0} = \frac{1}{2\beta^2} \left\{ \frac{d}{d\zeta} (b \cdot u_{c,g}) \right\}^i \quad \text{on } -c^i/2 \leq \zeta^i \leq c^i/2 \tag{3.12}$$

From thin airfoil theory for incompressible flow, making quasi-steady assumption, we can readily describe the volume source distribution along the blade chord as

$$s^i = 2 \frac{\partial \phi^i}{\partial \eta^i} \Big|_{\eta^i = 0} = \frac{1}{\beta^2} \left\{ \frac{d}{d\zeta} (b \cdot u_{c,g}) \right\}^i \tag{3.13}$$

Since

$$s^i = \frac{4\pi\beta^3}{\nu c} s(\zeta)$$

the corresponding source distribution in the compressible plane can now be written as

$$s(\zeta) = \frac{d}{d\zeta}\,(b \cdot u_{c,g}) \qquad (3.14)$$

and we note that the source distribution under the assumption $u_{c,g} << a_o$, is the same as that for an incompressible flow. Substituting from Eq. (3.4) for $u_{c,g}$, we obtain the source distribution $s_{g,j,\zeta}$ at ζ on the jth blade as

$$s_{g,j,\zeta} = \int_{-\infty}^{\infty} \hat{u}_{c,g}(\omega) \cdot e^{-i\phi_g} \cdot \exp\{-ig2\pi\tfrac{j-1}{B}\}$$

$$\times \exp\{-i(g\Omega+\omega)(t - \tfrac{\zeta}{V})\} \cdot \{\frac{db}{d\zeta} + ibg\Omega/V\}\, d\omega$$

For a blade element of span dr, we can consider the source $s_{g,j,\zeta} \cdot d\zeta dr$ concentrated at ζ, $\theta_{j,\zeta}$ and represent it by a complex Fourier series in θ. From the source distribution over an elemental volume $r_o\, d\theta_o \cdot dr_o \cdot d\zeta_o$ located at (r_o, θ_o, ζ_o), we obtain the source strength at r_o due to thickness of the jth blade element as

$$S_{g,j}(r_o) = \int_{-\infty}^{\infty} \hat{u}_{c,g}(\omega) \cdot e^{-i\phi_g} \exp\{-ig2\pi\tfrac{j-1}{B}\}$$

$$\times \sum_{m'} \frac{1}{2\pi} \exp\{-im'(\theta_o - \Omega t - 2\pi\tfrac{j-1}{B} + \frac{\Omega\zeta_o}{V})\}$$

$$\times \exp\{-i(g\Omega + \omega)(t-\zeta_o/V)\}$$

$$\times \{db/d\zeta_o + ibg\Omega/V\} \cdot d\zeta_o dr_o d\theta_o\, d\omega \qquad (3.15)$$

In summing the right hand side of Eq.(3.15) over j from 1 to B to take into account all the rotor blades, we note that

$$\sum_{j=1}^{B} \exp\{-i(g-m')2\pi\frac{j-1}{B}\} = B$$

for $(g-m') = nB$ with $n = \ldots -2,-1,0,1\ldots\ldots$ and zero otherwise. Consequently, the effect of thickness of the rotor blades on noise generation can be examined by considering the influence of the monopoles

$$S_g(r_o) = \frac{B}{2\pi}\int_{-\infty}^{\infty} \hat{u}_{c,g}(\omega)\cdot e^{-i\phi_g}\cdot\sum_{m'} e^{im'\theta_o}$$

$$\times \exp\{-i(nB\Omega+\omega)(t-r_o/V)\}$$

$$\times \{db/d\zeta_o + ibg\Omega/V\}\, d\zeta_o dr_o d\theta_o\, d\omega \qquad (3.16)$$

(b) Fluctuating Blade Loading and Resulting Dipole Sources:

Due to the fluctuations of the velocity component normal to the chord, there is fluctuating lift distribution along the blade chord. As in the preceding subsection, we first solve the problem in the equivalent incompressible plane and then obtain the result in the compressible case, following the analysis given by Osborne (Ref. 5). We introduce a convenient variable

$$\delta = \cos^{-1}(2\zeta/c)$$

to obtain the following expression for the vorticity distribution as a function δ on the jth blade due to its interaction with the velocity component $u_{\perp,g}$.

$$\gamma_{g,j}(\delta)\cdot\sin\delta = \frac{2}{\beta}\int_{-\infty}^{\infty}\hat{u}_{\perp,g}(\omega)\, e^{-i\phi_g}\, \exp\{-ig2\pi\tfrac{j-1}{B}\}$$

$$\times\ \exp(-i\nu t)\ \cdot\ \exp(-i\nu_R\cos\delta\, M^2/\beta^2)$$

$$\times\left\{\left[J_0(\nu_R/\beta^2) + iJ_1(\nu_R/\beta^2)\right]\right.$$

$$\times\left[\frac{K_1(-i\nu_R/\beta^2) + K_0(-i\nu_R/\beta^2)\cdot\cos\delta}{K_1(-i\nu_R/\beta^2) + K_0(-i\nu_R/\beta^2)}\right]$$

$$-\sum_{m=1}^{\infty}{}' i^{m-1}(\cos m\delta + \frac{i\nu_R}{m\beta}\sin\delta\,\sin m\delta)$$

$$\left.\times\left[J_{m-1}(\nu_R/\beta^2) + J_{m+1}(\nu_R/\beta^2)\right]\right\}d\omega \qquad (3.17)$$

where $\nu = (g\Omega+\omega)$; and $\nu_R = \nu c/2V$

The right hand side of the above equation can also be represented as

$$= \int_{-\infty}^{\infty} \hat{u}_{\perp,g}(\omega)\ e^{-i\phi g}\cdot\exp\{-ig2\pi\frac{j-1}{B}\}\cdot\gamma(\delta,\omega)$$
$$\chi\ \exp\{-i\ (g\Omega+\omega)t\}d\omega \qquad (3.18)$$

where $\gamma(\delta,\omega)$ is a complex function dependent only upon the reduced frequency and Mach number..

The lift fluctuation $dl_{g,j}$ at $(r,\theta_{j,\zeta},\zeta)$ acting on an elemental area $d\zeta\cdot dr$ of the jth blade can be expressed as

$$dl_{g,j} = \rho_o V\gamma_{g,j}(\zeta)\cdot d\zeta dr \qquad (3.19)$$

The force exerted by the blade on the fluid is equal and opposite to that given above, that is

$$df_{g,j} = -dl_{g,j} = -\rho_o V\gamma_{g,j}(\zeta)\cdot d\zeta dr \qquad (3.20)$$

Using complex Fourier series in θ, the concentrated force of Eq. (3.20) can be expressed as

$$df_{g,j} = -\frac{1}{2\pi}\sum_{m'}\rho_o V\cdot\exp\{-im'(\theta-\theta_{j,\zeta})\}\cdot\gamma_{g,j}(\zeta)\cdot d\zeta dr \qquad (3.21)$$

To include the effect of all the blades, the expression (3.21) is summed over j from 1 to B and we obtain the force acting on the medium due to an elemental volume $r_o d\theta_o dr_o d\zeta_o$ located at (r_o,θ_o,ζ_o) as

$$df_g(r_o) = -\frac{B}{2\pi}\int_{-\infty}^{\infty} \rho_o \hat{Vu}_{\perp,g}(\omega)\cdot e^{-i\phi_g}\,\gamma(\zeta_o,\omega)$$

$$\times \exp\{-i(nB\Omega+\omega)t\}$$

$$\times \sum_{m'} \exp\{-im\,\zeta_o\Omega/V\}\cdot e^{-im'\theta_o}\cdot d\zeta_o dr_o d\theta_o d\omega \quad (3.22)$$

where $g - m = nB$, $n = -\ldots-1,0,1\ldots\ldots$

The resulting acoustic dipole $D_g(r_o)$ at r_o and the force of $df_g(r_o)$ are related by

$$\rho_o\cdot\frac{\partial}{\partial t}\ (\vec{D}_g) = df_g$$

which gives $\vec{D}_g = \frac{-1}{i\rho_o k a_o}\ df_g(r_o)$ (3.23)

The components of the dipole in the axial and circumferential direction are given by

$$D_{g,z}(r_o) = -\int_{-\infty}^{\infty} \frac{i\sin\lambda\cdot dl_g(r_o,\omega)}{\rho_o k a_o}\cdot\exp\{-ika_o t\}\cdot d\omega \quad (3.24a)$$

$$D_{g,\theta}(r_o) = -\int_{-\infty}^{\infty} \frac{i\cos\lambda}{\rho_o k a_o} dl_g(r_o,\omega)\cdot\exp\{-ika_o t\}\cdot d\omega \quad (3.24b)$$

4.0 SOUND PROPAGATION IN THE DUCT AND RADIATION TO FARFIELD

In our earlier work reported in Ref. 1, we considered acoustic radiation from the sources in the rotor region to farfield, without any restrictions imposed by the surrounding duct. The analysis presented here is based on modal propagation of pressure waves in an annular duct with axial subsonic flow and radiation to farfield from the conditions occurring at the upstream end of the duct. Tyler and Sofrin (Ref. 6) suggest that the modes propagating in an infinitely long duct can be considered to yield the conditions occuring at the duct entrance. In the analysis presented here, we include the effect of finite distance between the rotor and the duct inlet and examine the influence of the impedence of the duct opening. In evaluating the latter, we assume that the duct terminates in an infinite flange and avoid the complicated computations employed by Lansing in Ref. (7) for the case of unflanged duct.

The modal propagation of acoustic waves due to an isolated source in an infinitely long duct is described in section 4.1, which is followed by a discussion of the integrated effect of the rotor-generated source distribution in 4.2. The effect of duct termination at a finite distance upstream of the rotor and acoustic particle velocities occuring at the duct-end are discussed in section 4.3. The method of calculating radiation to farfield and spectral density of farfield sound pressure level are described in section 4.4.

4.1 Pressure waves in an infinitely long annular duct due to source distribution in the rotor region.

Let us consider pressure waves propagating in an infinitely long annular duct due to monopole and dipole distributions given by Eq. (3.16) and (3.27) respectively. Following the analysis given in the Appendix, the pressure at r due to an elemental monopole $S_g(r_o)$ is given by

$$\Delta p_g^s(r) = (Bka_o\rho_o/2\pi\beta_o)\int_{-\infty}^{\infty} \hat{u}_{c,g}(\omega)e^{-i\phi_g}\sum_{m'} e^{-im'\theta_o}\exp(ika_o\zeta_o/V)$$

$$\times\sum_{m=-\infty}^{\infty}\sum_{\mu=0}^{\infty}\frac{1}{4\pi\Lambda_{m\mu}\frac{k\alpha}{\beta_o}}\, e^{im(\theta-\theta_o)}\, E_{m\mu}(r)\, E_{m\mu}(r_o)$$

$$\times \exp\{ik_z^{\pm}(z-z_o)\}\cdot\exp\{-ika_o t\}$$

$$\times \frac{db}{d\zeta_o}\, d\zeta_o\, dr_o\, d\theta_o\, d\omega \qquad (4.1)$$

and that due to dipole $\overset{+}{D}_g\ (r_o)$ is given by

$$\Delta p_g^d\ (r) = -\frac{B\rho_o V}{2\pi} \int_{-\infty}^{\infty} \hat{u}_{\perp,g}(\omega)\, e^{-i\phi_g}\, \gamma(\zeta_o,\omega) \sum_{m'} e^{-im'\theta_o}$$

$$\times \exp(-im'\zeta_o \Omega/V)$$

$$\times \sum_{m=-\infty} \sum_{\mu=0} \frac{\left\{\frac{m\cos\lambda}{\beta_o r_o} + k_z^{\pm} \sin\lambda\right\}}{4\pi \frac{k\alpha}{\beta_o} \Lambda_{m\mu}} e^{im(\theta-\theta_o)} E_{m\mu}(r) E_{m\mu}(r_o)$$

$$\times \exp\{ik_z^{\pm}(z-z_o)\} \cdot \exp(-ika_o t)$$

$$\times d\zeta_o\ dr_o\ d\theta_o\ d\omega \qquad (4.2)$$

where $k_z^{\pm} = \frac{k}{\beta_o^2}(\pm\alpha - M_o)$, $ka_o = (nB\Omega+\omega)$

and $\alpha = \{1 - (\beta_o k_{m\mu}/k)^2\}^{\frac{1}{2}}$

In equations (4.1) and (4.2), upper sign is chosen for downstream propagation and the lower sign is chosen for upstream propagation.

The effect of all the sources in the rotor region is accounted for by integrating the right-hand side of Eq. (4.1) and (4.2) between the limits

$$r_h \leq r_o \leq r_t$$

$$0 \leq \theta_o \leq 2\pi$$

$$-c/2 \leq \zeta_o \leq c/2$$

where $\zeta_o = z_o/\cos\lambda$

In carrying out the integration over θ_o, we note that

$$\int_0^{2\pi} \exp\{-i(m+m')\theta_o\}d\theta_o = \begin{cases} 2\pi & \text{if } m=-m' \\ 0 & \text{otherwise} \end{cases}$$

Thus the $m\mu$th mode of the duct pressure at (r,θ,z) due to monopoles in the rotor region can be written as

$$p^s_{g,m\mu}(r) = \frac{B\rho_o a_o}{4\pi\alpha\Lambda_{m\mu}} \int_{-\infty}^{\infty}\int_{r_h}^{r_t} \hat{u}_{c,g}(\omega)e^{-i\phi_g}\cdot E_{m\mu}(r_o)\ I_b \times E_{m\mu}(r)\cdot\exp\{im\theta + ik_z^{\pm}z - ika_o t\}\, dr_o d\omega \tag{4.3}$$

where

$$I_b = \int_{-c/2}^{c/2} \exp\{i\zeta_o(ka_o/V - k_z^{\pm}\cos\lambda)\} \times \{\frac{db}{d\zeta_o} + ibg\Omega/V\}\, d\zeta_o \tag{4.4}$$

and that due to dipoles as

$$p^d_{g,m\mu}(r) = -\frac{B\rho_o}{4\pi\frac{k\alpha}{\beta_o}\Lambda_{m\mu}} \int_{-\infty}^{\infty}\int_{r_h}^{r_t} \hat{u}_{\perp,g}(\omega)Ve^{-i\phi_g} \times \{\frac{m\cos\lambda}{\beta_o r_o} + k_z^{\pm}\sin\lambda\}E_{m\mu}(r_o)\ I_\ell \times E_{m\mu}(r)\cdot\exp\{im\theta + ik_z^{\pm}z - ika_o t\}\, dr_o d\omega \tag{4.5}$$

where

$$I_\ell = \int_{-c/2}^{c/2} \gamma(\zeta_o,\omega)\cdot\exp\{i\zeta_o(\frac{m\Omega}{V} - k_z^{\pm}\cos\lambda)\}d\zeta_o \tag{4.6}$$

The Equations (4.3) and (4.5) can be written as

$$p_{m\mu} = \int_{-\infty}^{\infty} A_{m\mu}(\omega) \exp\{i(m\theta - ka_o t + k_z^{\pm} z)\} E_{m\mu}(r) d\omega \qquad (4.7)$$

where

$$A_{m\mu}(\omega) = \frac{B\rho_o a_o}{4\pi\alpha\Lambda_{m\mu}} \int_{r_h}^{r_t} \hat{u}_{c,g} \cdot e^{-i\phi_g} E_{m\mu}(r_o) I_b dr_o \qquad (4.7a)$$

for acoustic propagation due to monopole distribution in the rotor region, and

$$A_{m\mu}(\omega) = -\frac{B\rho_o}{4\pi \frac{k\alpha}{\beta_o} \Lambda_{m\mu}} \int_{r_h}^{r_t} \hat{u}_{\perp,g} V e^{-i\phi_g} \left(\frac{m \cos\lambda}{\beta_o r_o} + k_z^{\pm} \sin\lambda\right) \times E_{m\mu}(r_o) I_\ell dr_o \qquad (4.7b)$$

for acoustic propagation due to dipole distribution in the rotor region. The superscripts $^+$ and $^-$ respectively indicate wave propagation in the downstream and upstream regions of the sources.

The speed with which a mode propagates in the axial direction is given by $a_o k/k_z^{\pm}$. Since k_z depends upon α and M_o as given in Eq. (4.2), let us consider the various conditions governing wave propagation or decay.

a) mode wave number $k_{m\mu} < k/\beta_o$:

The value of α for this case is real and positive, leading to real values for $k_z^{\pm}$. Consequently, Eq. (4.7) indicates

that the modes propagate upstream without decay for all real and positive values of α. However, the propagation in the downstream direction takes place only when $\alpha > M_o$.

b) mode wave number $k_{m\mu} = k/\beta_o$:
The value of α for this case is zero, and we find that the mode propagates only in the upstream direction with a speed of $(a/M_o)(1-M_o^2)$.

c) mode wave number $k_{m\mu} > k/\beta_o$:
For this case we can write

$$k_z' = \frac{k}{\beta_o^2}(\pm i\alpha - M_o)$$

with $\alpha = |1-(\beta_o k_{m\mu}/k)^2|^{\frac{1}{2}}$

We find that the mode propagates only in the upstream direction. However, the amplitudes of pressure and axial perturbation velocity in the mode would decay as $\exp\{k\alpha z/\beta^2\}$, where z is the distance from the rotor and is negative in the upstream region. Since α increases with the mode order, we note that higher order modes decay at a faster rate.

4.2 Effect of duct termination upstream of rotor.

Let us now consider the situation that the duct has infinite length on the downstream side but is terminated at a location $z = -\ell$, upstream. The $m\mu$th mode of pressure wave in the upstream direction due to sources in the rotor region is given by

$$p^-_{m\mu} = \int_{-\infty}^{\infty} A^-_{m\mu}(\omega) \cdot \exp\{i(m\theta - ka_o t + k^-_z z)\} \cdot E_{m\mu}(r) d\omega$$

$$= \int_{-\infty}^{\infty} p^-_{m\mu}(\omega) d\omega \qquad (4.8)$$

where $A^-_{m\mu}(\omega)$ corresponds to superscript (-) in Eqs. (4.7a) and (4.7b). Depending upon the impedence of the open end, the pressure waves will be reflected and travel back giving rise to right-running waves in this region upstream of the rotor. The pressure in each $m\mu$th mode of such reflected waves can be described by

$$p^+_{m\mu} = \int_{-\infty}^{\infty} A^+_{m\mu}(\omega) \cdot \exp\{im\theta - ika_o t + ik^+_z (z+\ell)\} \cdot E_{m\mu}(r) d\omega$$

$$= \int_{-\infty}^{\infty} p^+_{m\mu}(\omega) d\omega \qquad (4.9)$$

where A^+ is a complex constant which depends upon A^-, ℓ, and the impedence of the open end. The superscript (+) denotes that the above equation applies to the reflected right-running waves. We note that z is measured from the rotor, whereas the origin of these right-running waves is at the open end given by $z = -\ell$.

The axial acoustic perturbation velocity $u^{\pm}$ due to pressure waves given by (4.8) or (4.9) is evaluated from the linearized momentum equation in z direction

$$\frac{\partial}{\partial t}u^{\pm} + U \frac{\partial}{\partial z}u^{\pm} = -\frac{1}{\rho_o}\frac{\partial}{\partial z}p^{\pm} \tag{4.10}$$

where U is the mean axial velocity of the stream. Using Eqs. (4.8) and (4.9) for $p^{\pm}$ we obtain

$$u^{\pm}_{m\mu}(\omega') = \frac{k^{\pm}_z}{k - M_o k'_z} \frac{p^{\pm}_{m\mu}(\omega)}{\rho_o a_o}$$

$$= \frac{1}{\chi'} \frac{p'_{m\mu}(\omega)}{\rho_o a_o}, \text{ with } \chi' = \frac{k - M_o k'_z}{k'_z} \tag{4.11}$$

The factor χ' is termed as the "specific modal impedence ratio."

The perturbation velocities in the circumferential and radial directions are not considered since they do not carry acoustic energy across a transverse section of the duct.

To determine the pressure and velocity at the duct termination at z = -ℓ, resulting from an $m\mu$th mode of left running pressure wave, we follow the method suggested by Morse in Ref 8 and elaborated by Kaji in Ref. 9. We assume that the duct is terminated at z = -ℓ by an infinite transverse flange, but extends to infinite length in the positive z direction as shown in Fig. 2. Considering a single $m\mu$th mode of fluctuating distribution of axial velocity of the type

$$u_{m\mu} = \hat{u}_{m\mu} \cdot E_{m\mu}(r) \cdot \exp\{-i(ka_o t - m\theta)\}$$

over the annulus $r_h \leq r \leq r_t$,

it is shown in Ref. 9 that the resulting pressure distribution over the annulus can contain other radial modes than $E_{m\mu}(r)$. In terms of modal representation, we obtain

$$p_{m\mu} = -\rho_o a_o \hat{u}_{m\mu} \cdot \exp\{-i(ka_o t - m\theta)\} \times \sum_{\nu=0}^{\infty} \zeta_{m\nu}^{\mu} E_{m\nu}(r) \tag{4.12}$$

The subscript ν indicates all the radial modes resulting from the radial mode μ describing $u_{m\mu}$. The open-end radiation impedence ratio $\zeta_{m\nu}^{\mu}$ is discussed in detail in Ref. 9, and is given by

$$\zeta_{m\nu}^{\mu} = \frac{ik}{\Lambda_{m\nu}} \int_0^{\infty} \frac{I_{m\mu}(\tau)\ I_{m\nu}(\tau)}{(\tau^2 - k^2)^{\frac{1}{2}}} \tau d\tau$$

where $\Lambda_{m\nu} = \int_{r_h}^{r_t} \{E_{m\mu}(r)\}^2 \cdot r dr$

and $I_{m\mu}(\tau) = \int_{r_h}^{r_t} J_m(\tau r) \cdot E_{m\mu}(r) \cdot r dr$ (4.13)

Based on coupling impedences $\zeta_{m\nu}^{\mu}$ computed for a plane wave by Morse in Ref. 8, we assume

$$\zeta_{m\nu}^{\mu} << \zeta_{m\mu}^{\mu}$$

to simplify Eq. (4.12) to

$$p_{m\mu} = -\rho_o a_o \cdot u_{m\mu} \cdot \zeta_{m\mu}^{\mu} \tag{4.14}$$

Noting that the pressures and velocities at $z = -\ell$ in the above equation are obtained by summing the left-running and right-running waves, we obtain

$$\frac{p^-_{m\mu}(\omega) + p^+_{m\mu}(\omega)}{u^-_{m\mu}(\omega) + u^+_{m\mu}(\omega)} = -\rho_o a_o \zeta^\mu_{m\mu} \tag{4.15}$$

Substituting for $p^\pm_{m\mu}(\omega')$ from Eq. (4.11) into the above, we get

$$\frac{u^+_{m\mu}(\omega)}{u^-_{m\mu}(\omega)} = -\frac{\chi^- + \zeta^\mu_{m\mu}}{\chi^+ + \zeta^\mu_{m\mu}} \tag{4.16}$$

Using Eq. (4.11) we can also obtain

$$\frac{p^+_{m\mu}(\omega)}{p^-_{m\mu}(\omega)} = \frac{\chi^+ u^+_{m\mu}(\omega)}{\chi^- u^-_{m\mu}(\omega)} \tag{4.17}$$

We note that $\chi^\pm$ and $\zeta^\mu_{m\mu}$ are functions of ω .

At high frequency i.e., when $k \to \infty$:

$$\alpha \to 1, \quad k_z^\pm \to \frac{k}{\beta_o^2}(\pm 1 - M_o)$$

$$\chi^\pm \to \pm 1 \text{ and } \zeta^\mu_{m\mu} \to 1$$

then we note from Eq. (4.16) and (4.17) that both

$$\frac{u^{+}_{m\mu}(\omega)}{u^{-}_{m\mu}(\omega)} \quad \text{and} \quad \frac{p^{+}_{m\mu}(\omega)}{p^{-}_{m\mu}(\omega)} \to 0$$

which means that the $m\mu$th mode passes through the open end without reflection. However, at frequencies near cut-off i.e. when $k \to \beta_o k_{m\mu}$ from above:

$$\alpha \to 0, \quad k_z^{\pm} \to -\frac{kM_o}{\beta_o^2} \quad \text{and} \quad \chi^{\pm} \to -\frac{1}{M_o}$$

then we note from Eq. (4.16) and (4.17) that both

$$\frac{u^{+}_{m\mu}(\omega)}{u^{-}_{m\mu}(\omega)} \quad \text{and} \quad \frac{p^{+}_{m\mu}(\omega)}{p^{-}_{m\mu}(\omega)} \to -1$$

which means that the $m\mu$th modes near cut-off do not pass through the open end and are completely reflected back into the duct.

At intermediate frequencies the value of $\zeta^{\mu}_{m\mu}$ plays an important role in defining the conditions at the duct entrance based on which we can estimate the acoustic radiation to farfield. For example, the velocity fluctuation at $z = -\ell$ in the $m\mu$th mode given by

$$u_{m\mu}(\omega) = u^{-}_{m\mu}(\omega) + u^{+}_{m\mu}(\omega)$$

reduces to

$$u_{m\mu}(\omega) = \frac{\chi^+ - \chi^-}{\chi^+ + \zeta^{\mu}_{m\mu}} \quad \frac{p^-_{m\mu}(\omega)}{\rho_o a_o \chi^-}$$

using Eqs. (4.11) and (4.16).

ubstituting for $p^-_{m\mu}(\omega)$ fro. Eq. (4.8), we obtain

$$u_{m\mu}(\omega) = \int_{-\infty}^{\infty} \frac{A^-_{m\mu}(\omega)}{\rho_o a_o \chi^-} \quad \frac{\chi^+ - \chi^-}{\chi^+ + \zeta^{\mu}_{m\mu}}$$

$$\chi \exp\{i(m\theta - ka_o t - k_z^- \ell)\} \cdot E_{m\mu}(r) \cdot d\omega \qquad (4.18)$$

We note that velocity $u^-_{m\mu}$ in the $m\mu$th mode travelling upstream to the duct entrance together with reflection due to impedence $\zeta^{\mu}_{m\mu}$, gives rise to the resultant velocity $u_{m\mu}$ given in the above equation.

4.3 Far Field Radiation from the Duct Opening.

In the preceeding subsection,we calculated the $m\mu$th mode of axial acoustic velocity at the duct opening due to sources in the rotor region taking into account the impedence of the duct opening. To calculate the far-field pressure at a point (R, Ψ) as shown in Fig. 2, we follow the method suggested by Tyler and Sofrin in Ref. 6. The radiation at (R, Ψ) is considered to be that from distributed monopoles of strength $2u_{m\mu} r\, d\theta\, dr$, the factor of 2 being due to the fact that radiation only to the outside of the flanged duct is considered. Tyler and Sofrin ignored reflections at the duct opening and used the velocity in the upstream travelling waves given by Eq. (4.11) to estimate these monopoles. In the following analysis, we included the duct open-end impedence and the resultant velocity given by Eq. (4.18).

The farfield pressure at a point (R, Ψ) due to a source of strength $2u_{m\mu} r\, d\theta\, dr$ and curcular frequency ka_0 located at $(-\ell, \theta, r)$ is given by

$$\Delta P_{m\mu}(R, \Psi) = \int_{-\infty}^{\infty} -ika_0\rho_0 \{2u_{m\mu}(\omega) r\, d\theta dr\} \frac{e^{ikh}}{4\pi h}\, d\omega \qquad (4.19)$$

From Fig. 2, we note that the distance h from the source is given by

$$h = \{R^2 + r^2 - 2rR \sin\psi \cos\theta\}^{\frac{1}{2}}$$

$$\simeq R - r \cos\theta \sin\Psi, \text{ for small values of } r/R.$$

The pressure at (R, Ψ) due to all the distributed monoples at the duct opening is given by integrating (4.19) over the area of the duct and we obtain

$$P_{m\mu}(R, \Psi) = \int_{-\infty}^{\infty} \int_{r_h}^{r_t} \int_{0}^{2\pi} -ika_o\rho_o \cdot \frac{e^{ikh}}{4\pi h} \; 2u_{m\mu}(\omega) \; r \, d\theta \, dr \, d\omega \tag{4.20}$$

Substituting the value of h in the above equation, and ignoring higher order terms we get

$$P_{m\mu}(R, \Psi) = \int_{-\infty}^{\infty} \int_{r_h}^{r_t} \int_{0}^{2\pi} (-ika_o\rho_o) \cdot \frac{u_{m\mu}(\omega)}{2\pi R}$$

$$\chi \exp\{ikR - ikr \sin\Psi \cos\theta\} \cdot r \, d\theta \, dr \, d\omega \tag{4.21}$$

Substituting Eq. (4.18) for $u_{m\mu}$ into the above Equation and noting that

$$\int_{0}^{2\pi} \exp\{i(m\theta - kr \sin\Psi \cos\theta)\} \, d\theta = (-i)^m \, 2\pi J_m(kr \sin\Psi)$$

the Equation (4.21) becomes

$$P_{m\mu}(R, \Psi) = \int_{-\infty}^{\infty} (-i)^{m+1} \frac{k}{R\chi^-} \frac{\chi^+ - \chi^-}{\chi^+ + \zeta_{m\mu}^{\mu}} A_{m\mu}^{-}(\omega) \cdot I_{m\mu}(k \sin\Psi)$$

$$\chi \exp\{i \, (kR - ka_o t - k_z^- \ell)\} \, d\omega \tag{4.22}$$

where $I_{m\mu}(k \sin\Psi) = \int_{r_h}^{r_t} J_m(kr \sin\Psi) \cdot E_{m\mu}(r) \; r \, dr,$

a notation previously employed in evaluating $\zeta_{m\mu}^{\mu}$.

The total pressure at (R, Ψ) due to all the (m,μ) modes propagating in the annulus is given by

$$P(R, \Psi) = \sum_{m=-\infty}^{\infty} \sum_{\mu=0}^{\infty} P_{m\mu} \tag{4.23}$$

We note that the mean square value of pressure given above is equal to the integral of its spectral density. Hence,

$$\int \Phi_p(\nu)\, d\nu = \overline{P^2} = \overline{PP^*} \tag{4.24}$$

where $\nu = ka_o = nB\Omega+\omega$

and $\mu = ...-1,0,1.....$

The right-hand side of above equation, defined by Eqs. (4.22) and (4.23) is a function of $(nB\Omega+\omega)$, and leads us to the computation of spectral density of farfield pressure at circular frequency ν , and we obtain

$$\phi_p^s(\nu) = \left\{f\ F^s\right\}^* \cdot \left\{f\ F^s\right\} \phi_{u_{c,g}}(\omega) \qquad (4.25)$$

due to monopole distribution in the rotor region and

$$\phi_p^d(\nu) = \left\{f\ F^d\right\}^* \cdot \left\{f\ F^d\right\} \phi_{u_{\perp,g}}(\omega) \qquad (4.26)$$

due to dipole distribution in the rotor region.

Where

$$f = \frac{(-i)^{m+1}\ k}{R\chi^-} \quad \frac{\chi^+ - \chi^-}{\chi^+ + \zeta_{m\mu}^{\mu}} \quad I_{m\mu}(k \sin\Psi), \qquad (4.27)$$

$$F^s = \frac{B\rho_o a_o}{4\pi\alpha\Lambda_{m\mu}} \int_{r_h}^{r_t} E_{m\mu}(r_o)\ I_b\ dr_o \qquad (4.28)$$

and

$$F^d = \frac{B}{4\pi\frac{k\alpha}{\beta}\ \Lambda_{m\mu}} \int_n^{r_t} V\left\{\frac{m\cos\lambda}{\beta_o r_o} + k_z^{\pm}\ \sin\lambda\right\} \cdot E_{m\mu}(r_o)\ I_\ell\ dr_o \qquad (4.29)$$

5.0 RESULTS OF COMPUTATIONS AND COMPARISON WITH EXPERIMENTAL MEASUREMENTS

Based on modal propagation within the duct and reflections at the open end, radiation to far field from the small scale fan is computed using the equations derived in the preceding sections. The small scale fan configuration is sketched in Fig. 1 and its detail description is given in Ref. 1. The results of such computations are discussed in this section, and are compared with measurements.

In our acoustic computations, the fan data and other physical quantities used are as follows:

B = 15, r_h = 0.249 ft., (7.59 cm) r_t = 0.598 ft., (18.23 cm) N = 125.3 rps

	hub	pitch	tip
Blade chord (c)	0.125 ft. (3.81 cm)	0.117 ft. (3.57 cm)	0.115 ft. (3.51 cm)
Stagger angle (λ)	48°	63°	69.8°

U = 83.5 ft/sec, (25.45 m/sec) ρ_o = 0.002378 slug/c.ft. (0.001226 gram/c.cm) a_o = 1128.6 ft/sec (344 m/sec)

The support spider located at 7 in. (17.78 cm) downstream of the rotor has 8 vanes of 1.625 in. (4.13 cm) chord and 0.25 in. (6.35 mm) thickness.

Restricting our attention to noise levels at blade passing frequency, we have

$$k = \frac{B\Omega}{a_o} = \frac{2\pi BN}{a_o} = 10.6 \text{ per ft.} \quad (34.33 \text{ per meter})$$

From upstream mode cut-off condition

$$k > \beta_o k_{m\mu},$$

we find that only the following $m\mu$ modes need be considered:

$m = -4,....-1,0,1,.....4$

$\mu = 0$

From the relation $g+m = B$, we note that each gth component gives rise to the corresponding mth mode. Consequently, the values of g need to be considered are between 11 and 19. For each of the $(m\mu)$ modes listed we computed the radiation impedence $\zeta^{\mu}_{m\mu}$ of the open end of the annular duct, using the method described in the preceding section. The real and imaginary parts of $\zeta^{\mu}_{m\mu}$ thus computed are shown in Fig.3 .

In the experiments carried out on Rao Fan-2 in the anechoic chamber at NASA-Ames Research Center, there are no discernable upstream disturbances except for turbulent fluctuations in the inflow. Consequently, we consider the random monopole and dipole distributions due to blade thickness and blade loading resulting from the interaction of the random velocity fluctuations with the rotor.

The turbulence measurements taken at the fan inlet(private communication from Mr. B. K. Hodder) indicated that the mean square value of velocity fluctuations in the axial direction was 0.75% of the axial velocity of 83.5 ft/sec. (25.45 m/sec) Nearly the

same intensity was measured for the velocity fluctuations along the circumferential direction. Consequently, for our acoustic computations we used

$$\{\overline{u_\perp^2}\}^{1/2} = \{\overline{u_c^2}\}^{1/2} = 0.6263 \text{ ft/sec.} \quad (0.1908 \text{ m/sec})$$

Based on measured auto-correlation function for axial velocity fluctuations and a "frozen-convected" assumption with a convection velocity of 83.5 ft/sec (25.45 m/sec), we obtained ℓ_z = 25 in. (0.635 m) for us in our computations of the turbulence spectrum. A value of ℓ_θ = 3 in. (7.62 cm) is assumed to conform with our earlier computations presented in Ref. 1. The spectra of the turbulent fluctuations, $\Phi_{u_{\perp,g}}$ and $\Phi_{u_{c,g}}$ are then computed from Eq. (2.9), for substitution in Eqs. (4.25) and 4.26). The mean square value of blade lift distribution computed from Eqs. (3.17) and (3.19) for ω=0, is shown in Fig. 4.

In the preceding section, we discussed the left and right running sound waves resulting from the acoustic sources in the rotor region, which in turn depend upon the random velocity fluctuations met by the blades. To examine the effect of the particle velocities in the pressure waves on the generation of the acoustic sources, we carried out the following calculations. Based only on $u_{\perp,g}$ (i.e., inflow turbulence) we obtained $u^-_{m\mu}$ from Eqs. (4.8) and (4.11), and then $u^+_{m\mu}$ from Eq. (4.16) for each value of g and corresponding mode ($m\mu$). Since these velocity components are random, one can compare only their spectral densities, which depend on radius due to the function $E_{m\mu}(r)$ in

in Eq. (4.7). From the behavior of $E_{m\mu}(r)$ for each of the $m\mu$th modes considered as shown in Fig. 5, we note that the velocities $u^{\pm}_{m\mu}$ are largest at tip radius. The spectral density of $\phi_{u_{\perp,g}}$ also is a function of radius as can be seen from Eq. (2.9). Consequently, we calculated $\phi_{u^-_{m\mu}}$, $\phi_{u^+_{m\mu}}$ and $\phi_{u_{\perp,g}}$ at $\omega = 0$, and $r = r_t$ and listed them in Table 1. We observe that $\phi_{u_{\perp,g}}$ dominates and similar situation can be expected, when we consider the outcome of monopole sources due to the velocity fluctuations $u_{c,g}$. Consequently, we can ignore the interaction of propagating sound waves with the blade row, and justify the use of Eqs. (4.25) and (4.26) with the corresponding values of $\phi_{u_{c,g}}$ and $\phi_{u_{\perp,g}}$.

From the blade loading based on the random fluctuations of $u_\perp$, we computed sound pressure spectrum according to Eq. (4.26) at distance $R = 7$ ft (2.13 m) and angle Ψ ranging from 0 to $\pi/2$. To reduce the amount of computational work, we restricted our attention to the spectral density at the blade passing frequency by setting $\omega = 0$ and $\nu = 2\pi BN$ in Eq. (4.26). The sound pressure levels thus computed are shown in Fig.6.

In computing noise from blade thickness effect according to Eq. (4.25), we used a blade profile described by its thickness distribution $b(\zeta)$ given as

$$\frac{2}{c}\, b(\zeta) = \text{constant} \cdot \left(1 + \frac{2\zeta}{c}\right) \left\{-\log\left(1 + \frac{2\zeta}{c}\right) + \log 2\right\};$$

$$\text{with} \quad -c/2 \leq \zeta \leq \frac{c}{2}$$

By choosing 0.27182 for the constant in the above equation, we obtain a profile with a rounded leading edge and a maximum thickness of 10% of chord occurring at 37% from leading edge. The source-sink distribution $s(\zeta)$ is obtained by substituting $b(\zeta)$ from the above equation and $u_{c,g}$ from Eq. (3.4) into Eq. (3.14). The results of our computations for farfield noise due to blade thickness effect are also shown in Fig. 6.

The SPL dB levels shown in Fig. 6 for noise from the blade loading and blade thickness are from the spectral density per Hz of the acoustic pressure at blade passing frequency. Since the fluctuations of $u_\perp$ and u_c are considered random, one can add the mean square values of sound pressures from these two contributions to obtain the combined effect. However, we observe that the noise contributed from blade thickness effect is negligible in comparison to that from blade loading.

The experimental data given in Ref. 2 show the spectral analysis obtained using 25 Hz band-width. From our previous computations of sharp peaks in sound pressure around the blade passing frequency, as reported in Ref. (1), we can assume that integration over a 25 Hz band-width leads to a spectral density 12.1 dB higher than those computed from Eq. (4.25) or Eq. (4.26) at the blade passing frequency. The sound pressure levels thus estimated are shown in Fig.6 along with the measured data. Apart from the noise level, which is proportional to turbulence intensity, the theoretical estimates do not show the strong directivity found in the measured data.

We also computed the acoustic radiation to farfield from the sources in the rotor region, completely ignoring the effect of the duct, for the sake of comparison. The sound pressure levels thus estimated are shown in Fig. 7 and we note that they do show the type of directivity observed in the experimental data.

The inability of our theory in predicting the directivity of noise from a ducted fan can be due to any or all of the following reasons:

(a) The effect of the confining duct and its finite length are examined in this report by considering the radiation impedence of an annular duct terminated by an infinite flange, as sketched in Fig. 2. The duct configuration used in the tests, shown in Fig. 1, is a cylindrical section upstream of the rotor, and is

annular downstream. The propagating modes, and the open-end impedence for each of these modes in such a duct configuration may be different from those considered in this report. Modelling the bell-mouth configuration of the fan inlet by an infinite flange can be yet a suitable method. Even though the computations for a plane wave (i.e., $m = \mu = 0$ mode) presented on page 472 of Ref. 10 show that the absence of the flange does not appr ciably alter the radiation impedence of the duct opening, there is no indication that similar behavior exists for higher order modes.

(b) An ($m\mu$)th mode incident on the open end of the duct can give rise to various other radial modes. These (m,ν)th modes irrespective of duct cut off conditions can affect radiation to far field. In our analysis we ignored all such cross-coupling of modes. Computations for a plane wave presented on page 336 in Ref. 8 show that there is negligible cross-coupling at high frequencies. However, there is no indication that cross-coupling can be assumed negligible for higher order modes.

(c) The strong directivity occuring in radiation from blade loading directly to farfield (as shown in Fig.6) appears to be due to the dipole nature of the sources. In evaluating the farfield radiation from conditions occuring at the duct entrance, we considered only the axial component of the acoustic particle velocity at the duct termination and the corresponding monopole sources. We have ignored the gradients of velocity, and thus lost the dipole character of the scurces. In particular, we have not included the tangential components of the particle velocity and its gradient in the conditions occuring at the duct opening.

6.0 CONCLUSIONS AND RECOMMENDATIONS

From the analyses and computational results presented in this report, the following conclusions can be made:

1. Consideration of chord-wise distribution of the blade lift loading is important in evaluating sound at wave lengths comparable to the blade chord.

2. The farfield noise, predicted under the assumption of an annular duct terminated by an infinite flange, does not show considerable directivity. On the contrary, experimental measurements indicate about 10 dB drop on the sideline from that on the axis.

3. Sound pressure levels computed for an axis point including the effect of finite duct length upstream of the rotor is comparable to those computed for a free rotor in the absence of a duct.

4. The acoustic particle velocities in pressure waves reflected at the duct opening are negligible compared to the inflow turbulent velocity fluctuations based upon which pressure waves propagating upstream towards the duct opening are calculated. consequently, the second order effect on sources in the rotor region due to interaction of the propagating pressure waves with rotor blades can be ignored.

Comparison of theoretical estimates with experimental measurements and a critical examination of the assumptions employed in our analysis lead us to the following recommendations for future effort in fan noise evaluation and reduction of far field noise.

1. Space-time correlation measurements of flow in the duct are of prime importance in making theoretical predictions of noise from the ducted rotor. The spectral density distribution of fluctuations of u_c and $u_\perp$ depend upon the measurements of ℓ_θ and the autocorrelation function. Even a small steady-state velocity deficit of 0.5 ft/sec (0.152 m/sec) when occurring over a small region of the fan inlet, can give rise to on axis-noise comparable to that presently estimated from the inflow turbulence. Detailed measurements at fan inlet, as suggested here, can detect such velocity distortions.

2. The assumption of an infinite flange at the opening of an annular duct is employed in our analysis to avoid complexity and excessive computational effort. Also, the "cross-coupling" of radial modes at the duct opening is assumed negligible. The discrepancy between the predicted and experimentally determined directivity patterns may be due to the above simplifying assumptions, and also partly due to some other noise sources overlooked in our analysis. Even though our primary interest is in reduction at its sources, modal transmission of acoustic

waves in ducts with cross-sectional discontinuity similar to that occurring in practice, and reflection of higher order modes at the duct opening requires further examination to formulate reliable fan noise prediction methods.

REFERENCES

1. Rao, G.V.R., Chu, W.T., and Digumarthi, R.V., "Theoretical Studies of Tone Noise from a Fan Rotor," NASA CR-2354, November 1973.

2. Hodder, B.K., "Investigation of the Effect of Inlet Turbulence Length Scale on Fan Discrete Noise," NASA TM X-62, 300, September 1973.

3. Madelung, E., "Die Mathematischen Hilfsmittel des Physikers," Julius Springer, Berlin, 1936, p. 28, Eq. (18), (also Dover Publications, 1943.)

4. Horlock, J. H., "Fluctuating Lift Forces on Aerofoils Moving through Transverse and Chordwise Gusts, "Journal of Basic Engineering, ASME Trans., December 1968, pp. 494-500.

5. Osborne, C., "Unsteady Thin Airfoil Theory for Subsonic Flow," AIAA Journal, Vol. 11, 1973, pp. 205-209.

6. Tyler, J.M., and Sofrin, T.G., "Axial Flow Compressor Noise Studies," S.A.E. Trans., Vol. 70, pp 309-332.

7. Lansing, D. L., "Exact Solution for Radiation of Sound from a Semi-Infinite Circular Duct with Application to Fan and Compressor Noise." Analytical Methods in Aircraft Aerodynamics, NASA Sp-228.

8. Morse, P.M., "Vibration and Sound, " McGraw-Hill, 1948.

9. Kaji, S., "Radiation of Rotational Noise of Turbo Machinery at Duct Opening," Trans. Japan Soc. Mech. Eng., Vol. 38, No. 315, November 1972.

10. Morse, P.M., and Ingard, K. Uno, "Theoretical Acoustics," McGraw-Hill, 1969.

APPENDIX

Pressure waves in an infinitely long annular duct due to an isolated source.

Let us consider a monopole source

$$S(t) = \hat{S} \cdot e^{-ik a_o t} \tag{A1}$$

inside an annular duct $r_h \leq r \leq r_t$ with an axial inflow velocity U_a.

The governing equation for pressure is the acoustic equation which has undergone a Galilean transformation since we have a moving fluid of subsonic Mach number $M_o = U_a/a_o$.

$$\frac{1}{a_o^2} \frac{\partial^2 p}{\partial t^2} - \nabla^2 p + \frac{2M_o}{a_o} \frac{\partial^2 p}{\partial z \partial t} + M_o^2 \frac{\partial^2 p}{\partial z^2} = \rho_o \frac{\partial S}{\partial t} \delta(r-r_o) \delta(\theta-\theta_o) \delta(z-z_o) \tag{A2}$$

where $\nabla^2 = \frac{\partial^2}{\partial r^2} + \frac{1}{r} \frac{\partial}{\partial r} + \frac{1}{r^2} \frac{\partial^2}{\partial r^2} + \frac{\partial^2}{\partial z^2}$

The right hand side of Equation (A2) represents the Lighthill source term. The boundary conditions on pressure are

$$\frac{\partial p}{\partial r} = 0 \quad \text{at } r = r_h \text{ and } r_t$$

Using the Lorentz transformation

$$r = R;\ \theta = \theta,\ z = \beta Z,\ t = (T - M_0 Z/a_0)/\beta_0$$

where $\beta_0^2 = 1 - M_0^2$, the Eq(4.2) can be written as

$$\frac{1}{a^2}\frac{\partial^2 p}{\partial T^2} - \left\{\frac{\partial^2}{\partial R^2} \cdot \frac{\partial}{\partial R} + \frac{1}{R^2}\frac{\partial^2}{\partial \theta^2} + \frac{\partial^2}{\partial Z^2}\right\} p$$

$$= -i\frac{k}{\beta_0} a_0 \rho_0 \hat{S} \cdot \delta(R-R_0)\,\delta(\theta-\theta_0)\,\delta(Z-Z_0) \cdot \exp\{-ika_0(T-M_0 Z/a_0)/\beta_0\} \tag{A3}$$

and the boundary conditions become

$$\frac{\partial p}{\partial r} = 0 \text{ at } R = r_h \text{ and } r_t.$$

We seek the solution of Eq. (A3) in the form

$$p^s = -i\frac{k}{\beta_0} a_0 \rho_0 \hat{S}\ g(R/R_0) \cdot \exp\{-ika_0 T/\beta_0\} \tag{A4}$$

where the Green's function $g(R/R_0)$ is defined in the transformed coordinates.

Substituting Eq. (A4) into Eq. (A3), we find that $g(R/R_0)$ satisfies the differential equation

$$\left\{\frac{\partial^2}{\partial R^2} + \frac{1}{R}\frac{\partial}{\partial R} + \frac{1}{R^2}\frac{\partial^2}{\partial \theta^2} + \frac{\partial^2}{\partial Z^2} + \frac{k^2}{\beta^2}\right\} g(R/R_0)$$

$$= -\delta(R-R_0)\,\delta(\theta-\theta_0)\,\delta(Z-Z_0) \cdot \exp\{ikM_0 Z/\beta_0\} \tag{A5}$$

and the boundary conditions

$$\frac{\partial g}{\partial R} = 0 \text{ at } R = r_h \text{ and } r_t. \tag{A6}$$

Solving Eq. (A5) subject to the boundary conditions (A6) by the method of separation of variables, we obtain

$$g(R/R_0) = \sum_{m=-\infty}^{\infty} \sum_{\mu=0}^{\infty} \frac{i}{4\pi \frac{k\alpha}{\beta_0} \Lambda_{m\mu}} e^{im(\vartheta-\theta_0)}$$

$$\times E_{m\mu}(R) E_{m\mu}(R_0) \cdot \exp(ikM_0 Z_0/\beta_0)$$

$$\times \exp\{\pm i \frac{k\alpha}{\beta_0} (Z-Z_0)\} \qquad \text{(A7)}$$

where

$$\alpha = \{1-(\beta_0 k_{m\mu}/k)^2\}^{\frac{1}{2}} ,$$

In Eq. (A7) we take + sign for the region downstream (on right) of source location while for the region upstream of source location (on left), the negative sign is chosen.

Rewriting in original variables, the Eq. (A7) becomes

$$g(r/r_0) = \sum_{m=-\infty}^{\infty} \sum_{\mu=0}^{\infty} \frac{i}{4\pi \frac{k\alpha}{\beta_0} \Lambda_{m\mu}} e^{im(\theta-\theta_0)}$$

$$\times E_{m\mu}(r) E_{m\mu}(r_0) \cdot \exp(ikM_0 z_0/\beta_0^2) \cdot \exp\{\pm i k\alpha (z-z_0)/\beta_0^2\}$$

(A8)

and the acoustic pressure at (r,θ,z) due to a monopole is given by

$$p^s(r,\theta,z) = -i\frac{k}{\beta_o}a_o\rho_o\,\hat{S}\cdot g(r/r_o)$$

$$\times \quad \exp(-ika_o t)\cdot\exp(-ikM_o z/\beta_o^2) \qquad (A9)$$

Let us now consider the acoustic pressure at (r,θ,z) due to a dipole $\vec{D}(t) = \hat{\vec{D}}e^{-ika_o t}$ at (r,θ,z), $\hat{\vec{D}}$ being the strength of the vector dipole and $ka_o = (nB\Omega+\omega')$.

The acoustic pressure due to dipole is easily determined by differentiating Eq. (4.4) in the direction of dipole axis and replacing the monopole strength by dipole strength. Thus we obtain

$$p^d(R) = i\frac{k}{\beta_o}a_o\rho_o\,\hat{\vec{D}}\cdot\nabla_o\, g(R/R_o)\exp(-ika_o T/\beta_o) \qquad (A10)$$

where

$$\nabla_o \equiv \hat{i}\frac{\partial}{\partial R} + \hat{j}\frac{\partial}{R_o\partial\theta_o} + \hat{k}\frac{\partial}{\partial Z_o}$$

Writing in original variables, Eq. (4.10) becomes

$$p^d(r) = -i\frac{k}{\beta_o}a_o\rho_o\left\{\hat{D}_r\cdot\frac{\partial g}{\partial r_o} + \hat{D}_\theta\cdot\frac{\partial g}{r_o\partial\theta_o} + \hat{D}_z\cdot\beta_o\frac{\partial g}{\partial z_o}\right\}$$

$$\times \exp(-ika_o t)\ \times \exp(-ikM_o z/\beta^2) \qquad (A11)$$

where $(\hat{D}_r, \hat{D}_\theta, \hat{D}_z)$ are the components of $\hat{\vec{D}}$ in r,θ and z directions respectively.

Table I. Spectral intensities of inflow turbulent velocities and the particle acoustic velocities in the propagating duct-modes.

Mode $m\mu$	$\Phi_{u_{\perp},g}$ (turbulence)	$\Phi_{u^-_{m\mu}}$ (incident on duct opening)	$\Phi_{u^+_{m\mu}}$ (reflected from duct opening)
(-4,0)	.430 (10^{-5})	1.121 (10^{-8})	.068 (10^{-8})
(-3,0)	.480 (10^{-5})	1.464 (10^{-8})	.227 (10^{-8})
(-2,0)	.584 (10^{-5})	1.638 (10^{-8})	.066 (10^{-8})
(-1,0)	.605 (10^{-5})	1.623 (10^{-8})	.067 (10^{-8})
(0,0)	.687 (10^{-5})	1.929 (10^{-8})	.130 (10^{-8})
(1,0)	.786 (10^{-5})	1.796 (10^{-8})	.074 (10^{-8})
(2,0)	.909 (10^{-5})	1.276 (10^{-8})	.049 (10^{-8})
(3,0)	1.063 (10^{-5})	2.280 (10^{-8})	.349 (10^{-8})
(4,0)	1.250 (10^{-5})	0.152 (10^{-8})	.009 (10^{-8})

Note: Φ_u above has units of $(ft/sec)^2$

one foot/sec = 0.3048 m/sec

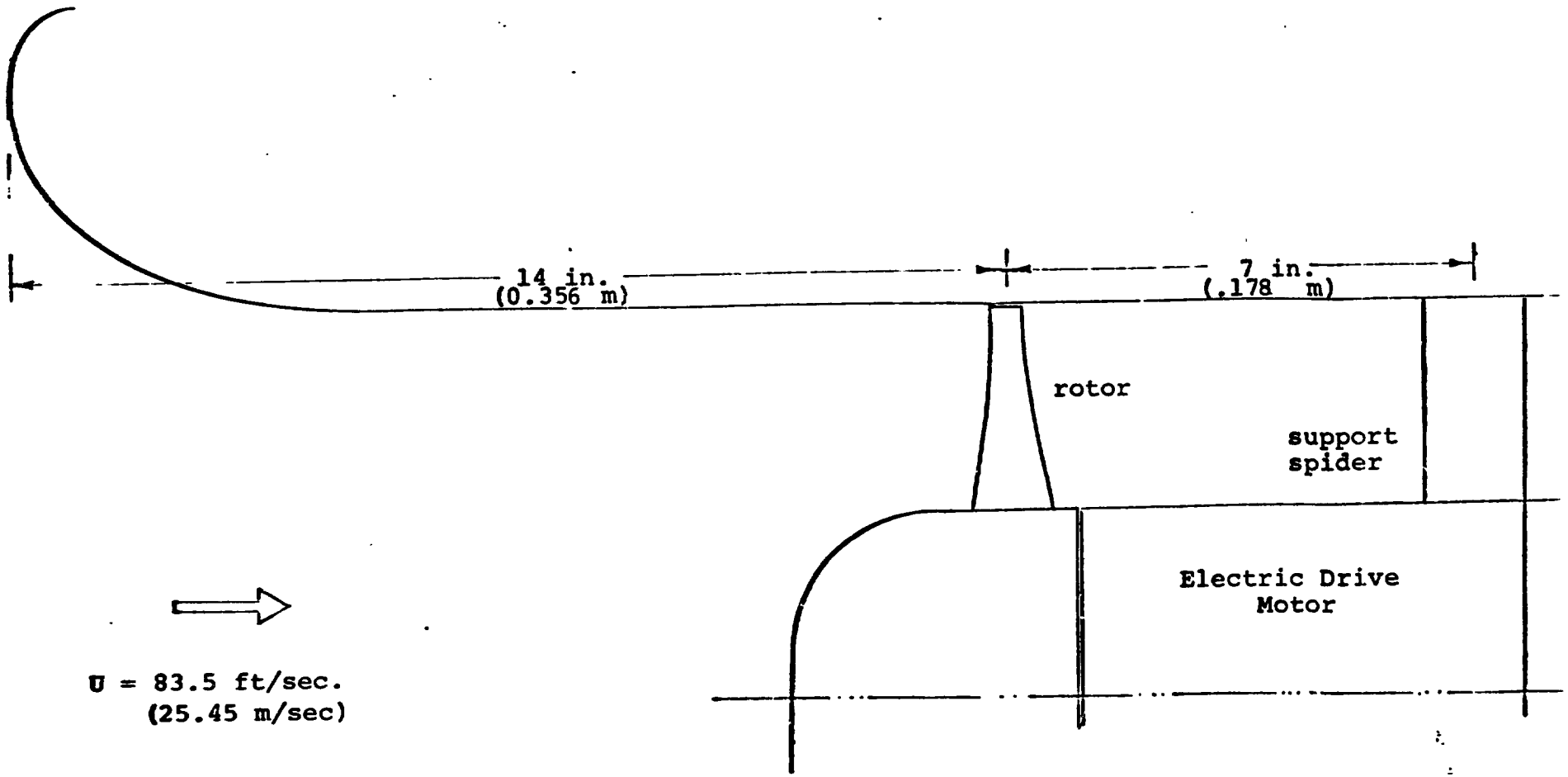

Fig. 1 Sketch of the Small Scale Fan used in The Test Program
(downstream duct extends to outside the chamber)

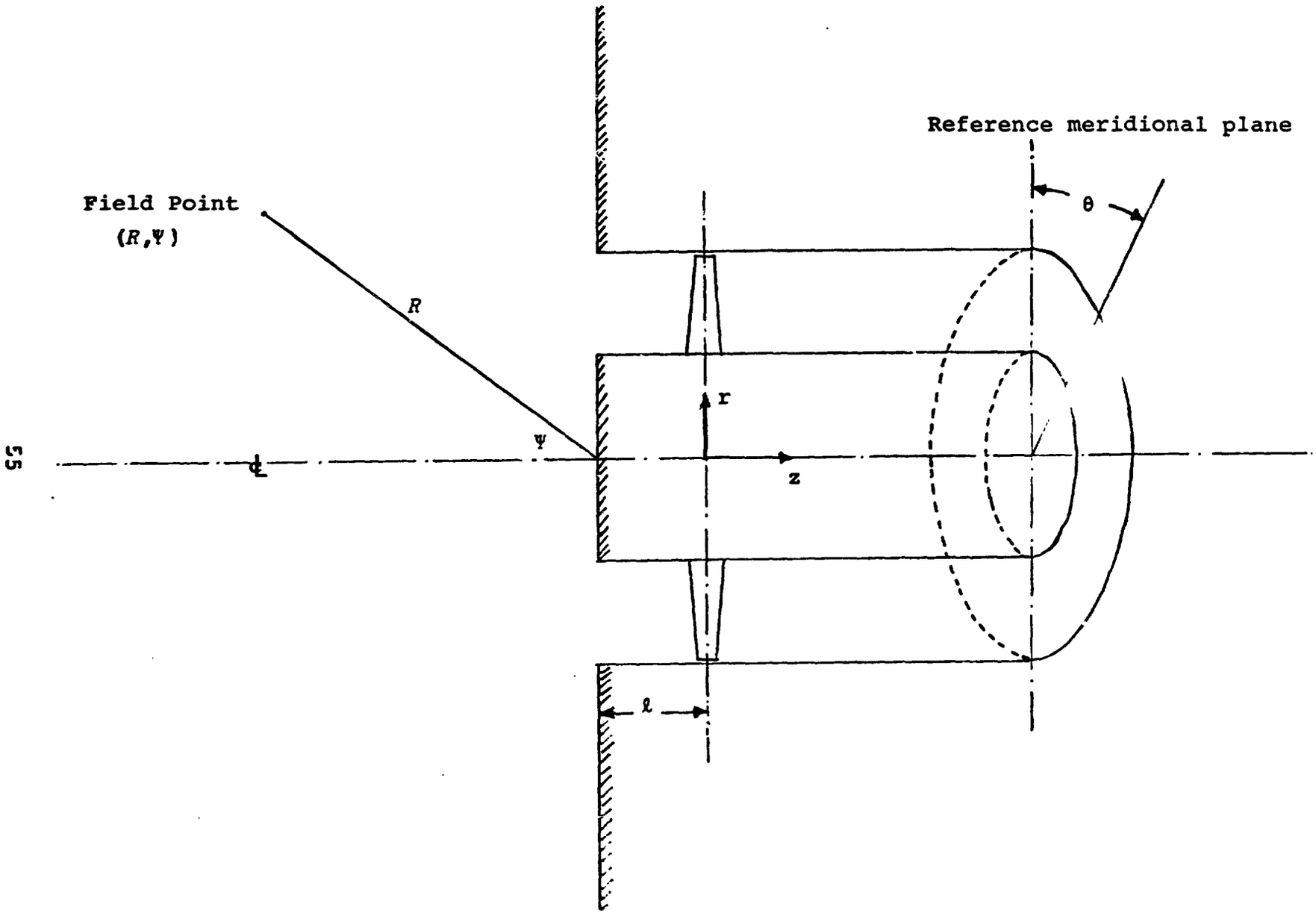

Fig. 2. Duct Configuration used in the Theoretical Analysis and Coordinate System.

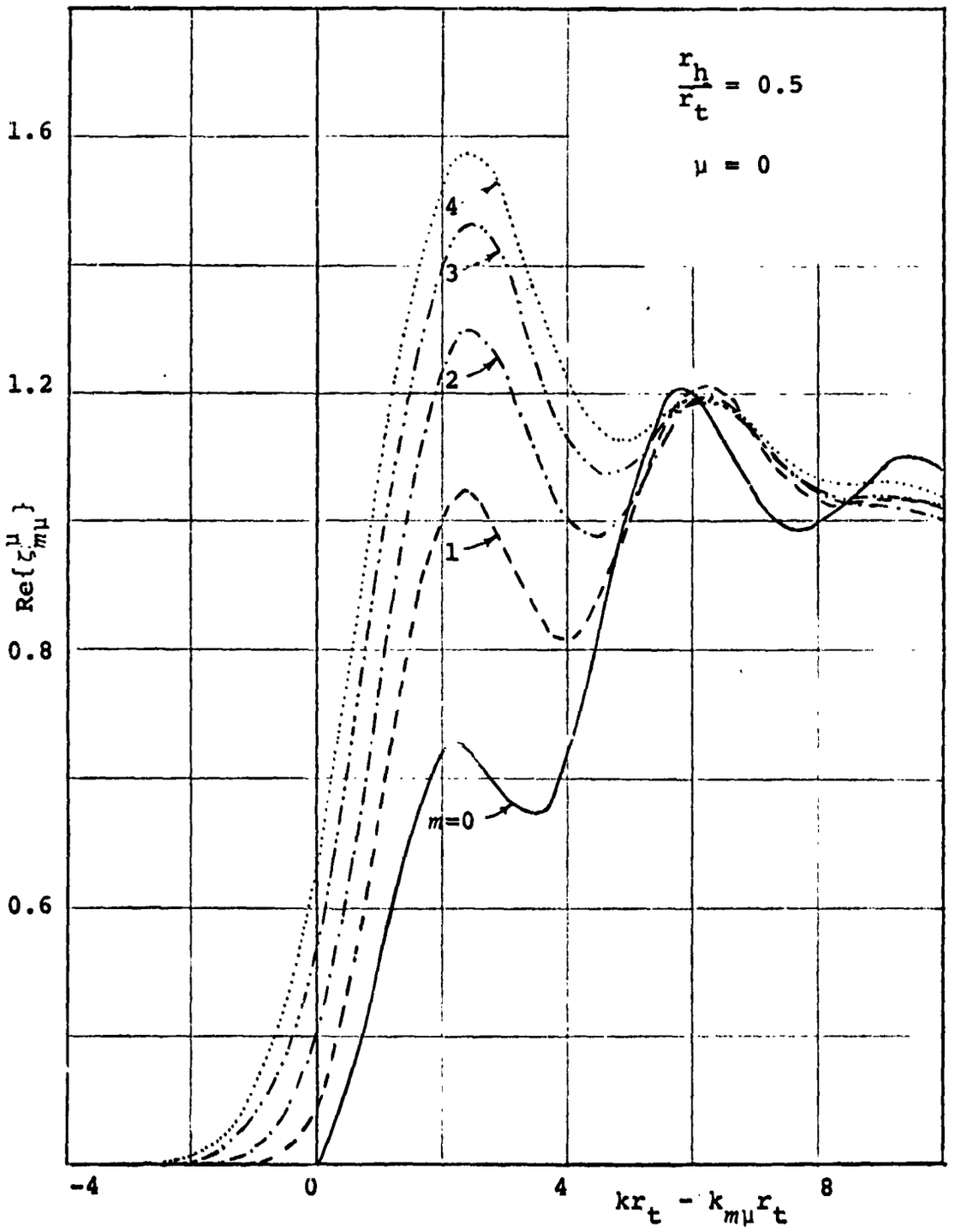

Fig. 3. Real Part of Radiation Impedence for the Flanged Open-end of an Annular Duct.

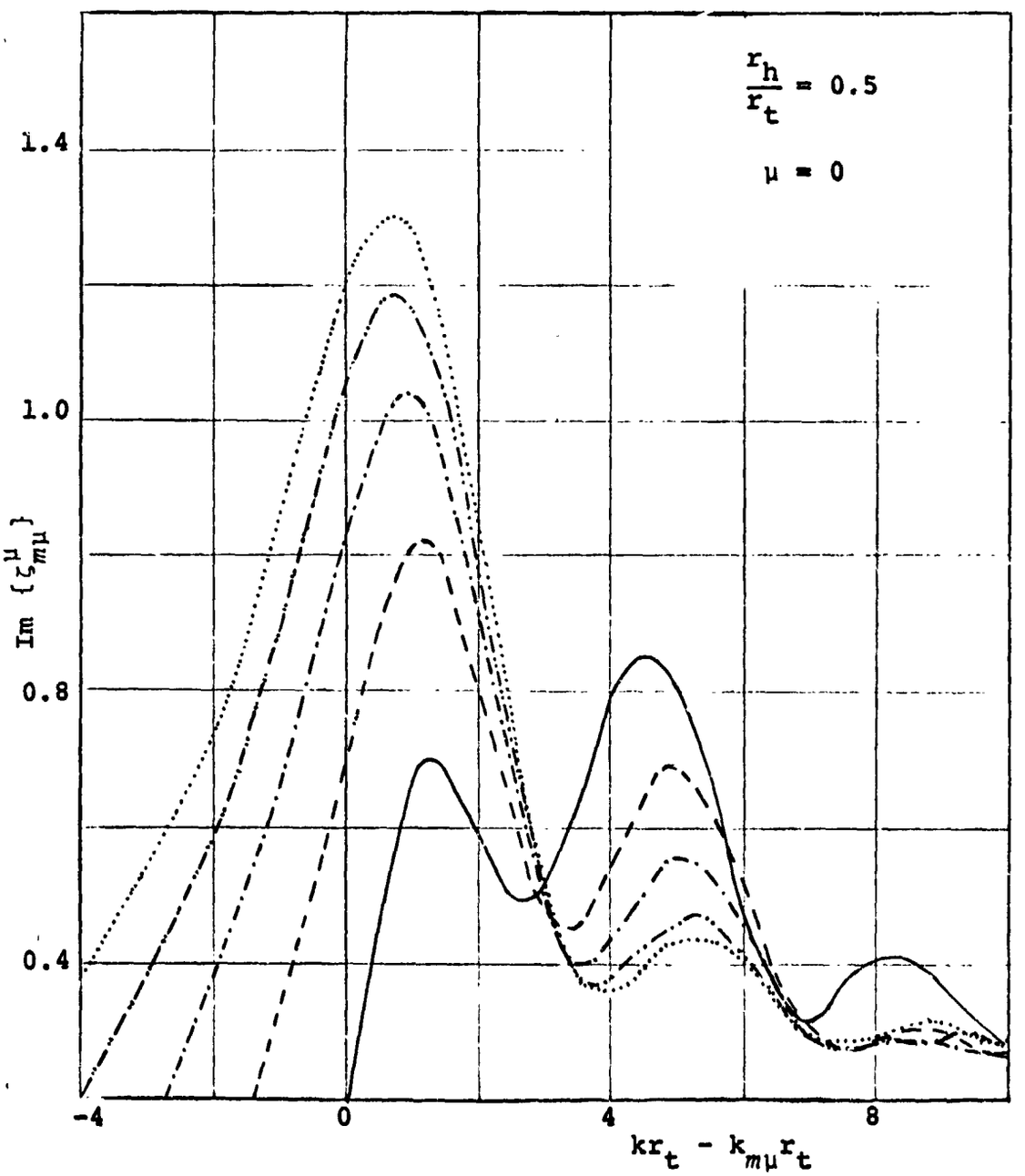

Fig. 3. Continued.

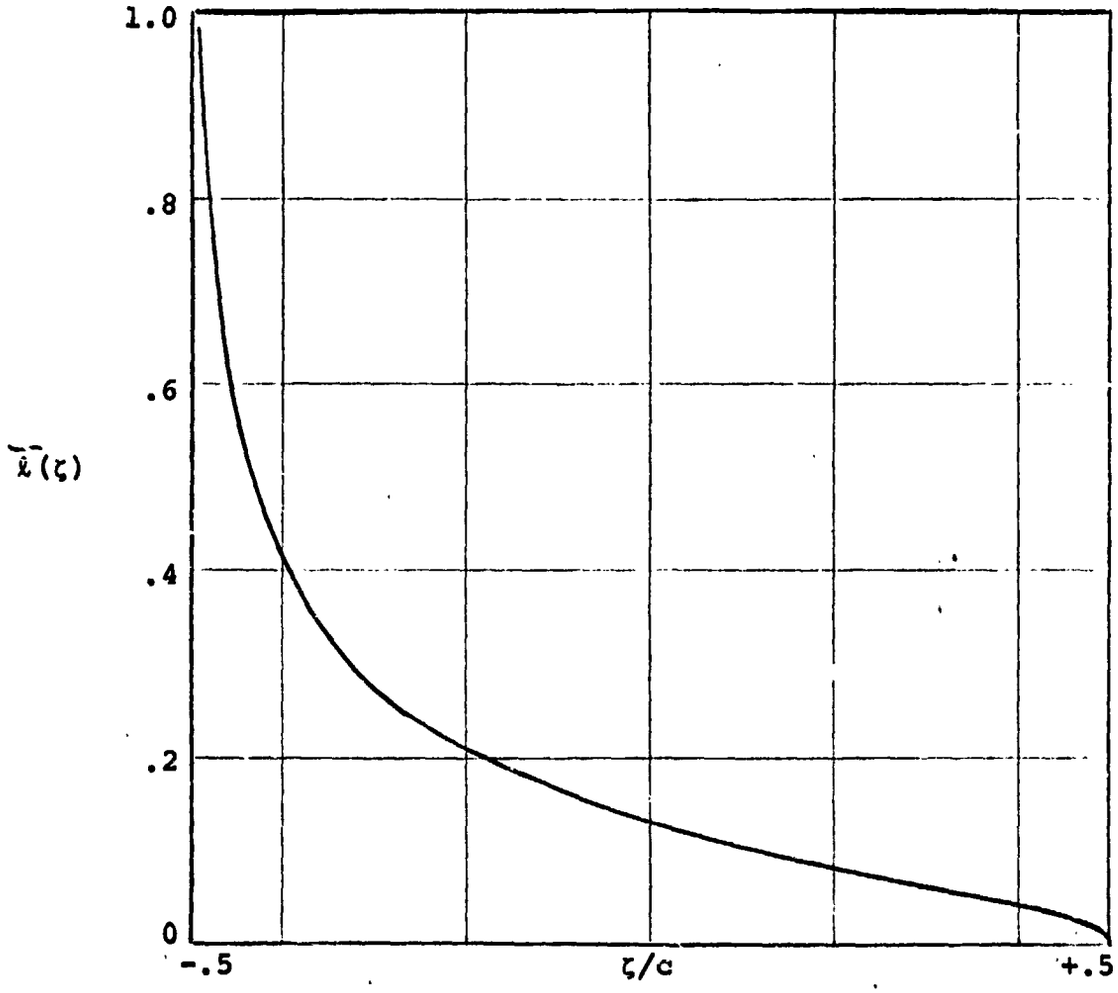

Fig. 4. Chord-wise Distribution of Lift on Rotor Blade.

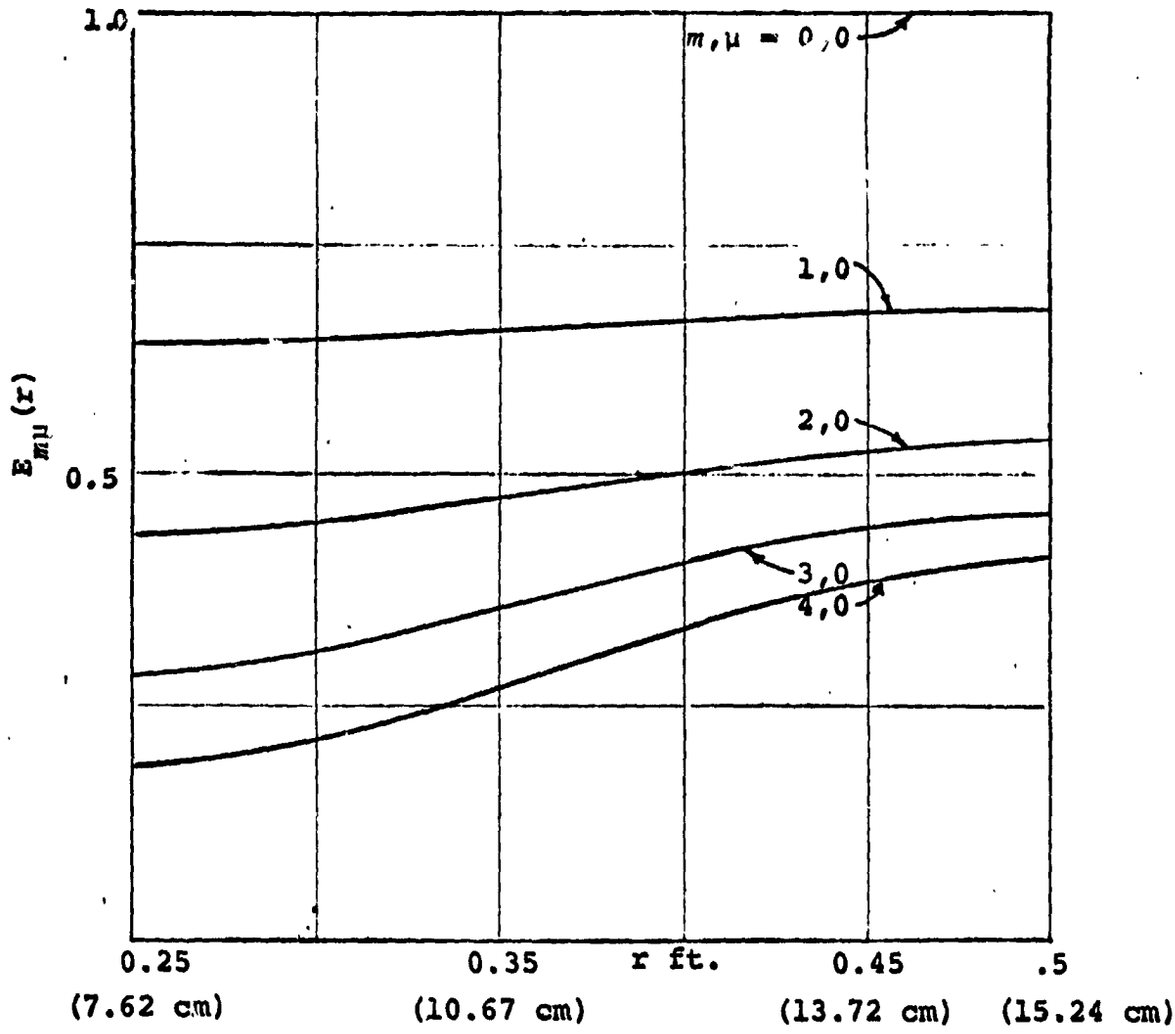

Fig. 5. Characteristic Functions $E_{m\mu}(r)$ for an Annular Duct (hub-tip ratio = 0.5).

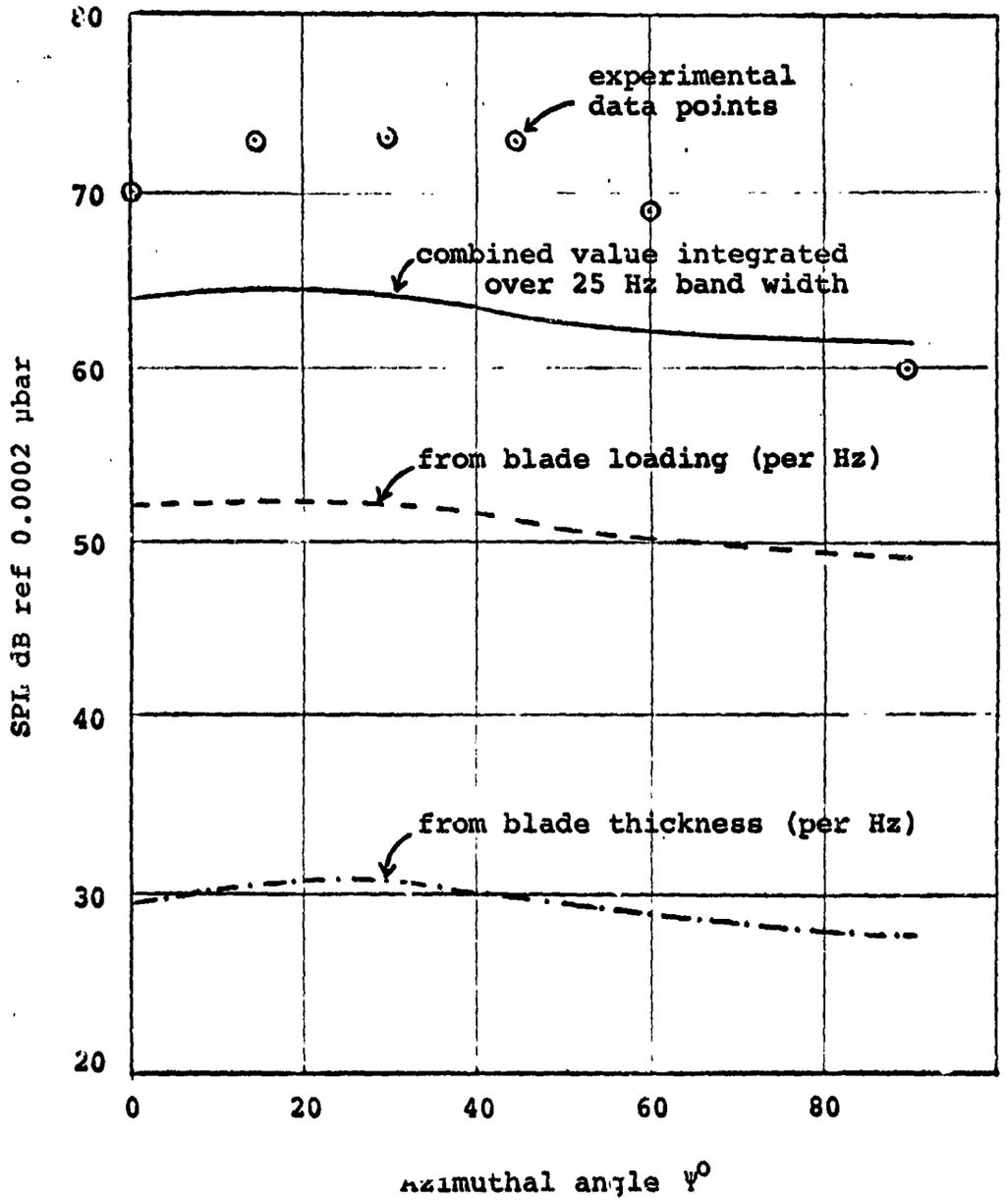

Fig. 6. Sound Pressure Levels at BPF at 7 ft. (2.13 m) from ducted Rotor, due to Inflow Turbulence.

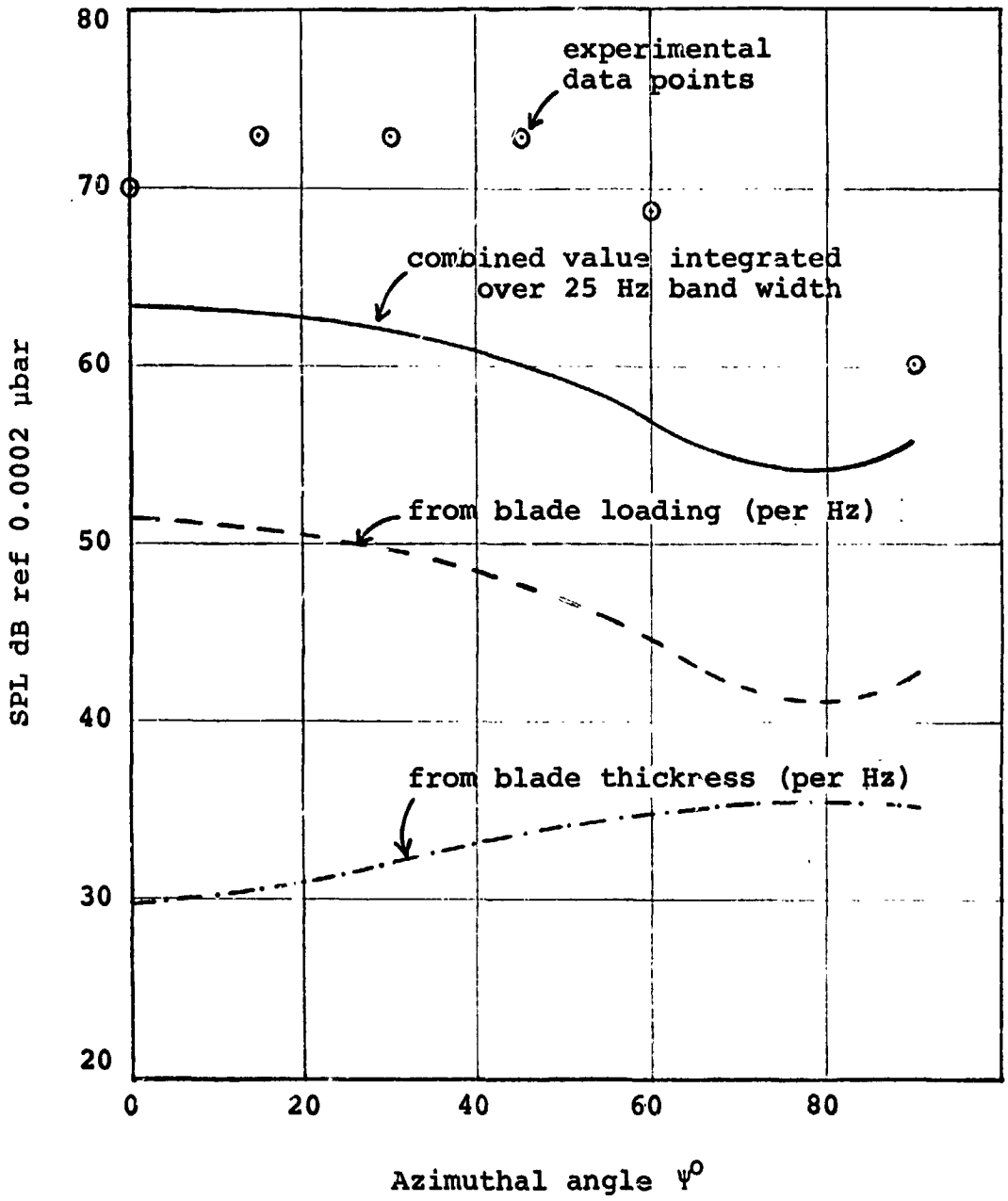

Fig. 7. Sound Pressure Levels at BPF at 7 ft. (2.13 m) from isolated Rotor due to Inflow Turbulence.